Honours Research Thesis

Project Title: Recapitulating Glial and Neuronal Development *In Vitro* for a Down's Syndrome Model of Alzheimer's Disease and a Model of Activity-Dependent Neuronal Epigenetic Reorganisation

Word Count: 7977

Student: Jack T. T. Goodrich[1,2]

Primary Supervisor: Ernst J. Wolvetang[1]

Co-Supervisor: Justin J. Cooper-White[2,3,4]

Assistant Supervisor: Dmitry A. Ovchinnikov[1]

Affiliations:

[1]Stem Cell Engineering Group, Australian Institute of Bioengineering and Nanotechnology, The University of Queensland, St Lucia, Brisbane, QLD, 4072, Australia

[2]Tissue Engineering and Microfluidics Group, Australian Institute of Bioengineering and Nanotechnology, The University of Queensland, St Lucia, Brisbane, QLD, 4072, Australia

[3]School of Chemical Engineering, The University of Queensland, St Lucia, Brisbane, QLD, 4072, Australia

[4]CSIRO Materials Science and Engineering, 37 Graham Rd, Highett, VIC, 3190, Australia

Statement of Authorship

I, Jack T. T. Goodrich, confirm that the work contained in this proposal has been produced solely by me, except where identified to the contrary*. I confirm that this work is my own and is being submitted in partial fulfilment of the requirements for the degree of Bachelor of Science (Honours) at The University of Queensland in 2013/2014 and has not been submitted anywhere else in any other form for the fulfilment of any other degree or qualification.

Word Count: 7977

Date: 15/5/2014

Signature: Jack T. T. Goodrich

(Jack T. T. Goodrich)

I, Ernst J. Wolvetang, confirm that I have seen a copy of the work presented in this research proposal/research report as the primary supervisor of Jack T. T. Goodrich.

Date: 15/5/2014

Signature: 

(Ernst J. Wolvetang)

Contents

List of Abbreviations

Aβ	Amyloid-β protein
AD	Alzheimer's disease
APP	Amyloid precursor protein
cDNA	Complementary deoxyribonucleic acid
DNA	Deoxyribonucleic acid
DNMT	DNA methyltransferase
DS	Down's syndrome
FACS	Fluorescence-activated cell sorting
MACS	Magnetic-activated cell sorting
FAD	Familial Alzheimer's disease
hESC	Human embryonic stem cell
hiPSC	Human induced pluripotent stem cell
ICC	Immunocytochemistry
IEG	Immediate early gene
NFT	Neurofibrillary tangles
PCR	Polymerase chain reaction
PDMS	Polydimethylsiloxane
qPCR	Quantitative polymerase chain reaction
RT	Room temperature (25°C)
RNA	Ribonucleic acid
SAD	Sporadic Alzheimer's disease
TCP	Tissue culture plastic
TUNEL	Terminal deoxynucleotidyl transferase dUTP nick end labelling

Abstract

Alzheimer's disease (AD) is a neurodegenerative disease affecting over 300,000 Australians with an estimated cost of $4.9billion per annum. Identification of novel therapeutic targets is essential for the development of effective therapies to prevent or treat AD. Models of Down's syndrome (DS) present an opportunity to study AD since 100% of DS patients develop AD by 40 years of age. Two important cell types that appear to be affected in the AD and DS brain are neurons and astrocytes. Using human induced pluripotent stem cells (hiPSCs) derived from DS patients is a valuable tool for such an investigation as it presents the only ethically viable option at present to model disease conditions in the brain with live human cells *in vitro*. One of the main disease phenotypes of AD is progressive memory and learning impairment. Memory and learning is thought to be directly driven in part by epigenetic changes in the neuronal genome. It has been postulated that the transmission and recording of neuronal activity can be imprinted by DNA methylation in the neuronal epigenome. The genes that regulate DNA methylation are known as DNA methyltransferases (DNMTs). These have been shown to be activated following neuronal activity. If we are to understand how memory and learning is epigenetically recorded in the neuronal genome, we must first understand how depolarisation affects the activity of these genes.

The aim of this project was thus two-fold. Firstly, to develop a faster and more efficient astrocyte differentiation protocol in hiPSCs in order to co-culture DS and control hiPSC-derived neruons and astrocytes to identify whether the AD phenotypes in DS neurons could be rescued with WT astrocytes. Secondly, we wanted to make mature, depolarisable hiPSC-derived neurons and determine whether neuronal activity would alter the activity of the methylation genes DNMT1, DNMT3a and DNMT3b. It was found that reproduction of astrocyte differentiation in culture proved difficult and unsuccessful. Mature neurons were however able to be characterised in order to have a defined population of cells in anticipation

of co-culture. We also showed that DNMT genes activity did not behave as expected, despite evidence that cells were in fact depolarising. This leaves much work to be done in interrogating the underlying mechanisms regulating DNA methylation in hiPSC-derived neurons. Fortunately, depolarised hiPSC samples are currently being assessed for activity-induced changes in DNA methylation, hydroxymethylation and non-CG methylation, as well as in the transcriptome, which will go far in shedding light on some of the mechanisms involved in the epigenetic changes elicited post neuronal depolarisation.

Acknowledgements

The following people must be acknowledged for their aid during this project in what was at times a harrowing journey but an invaluable life lesson: first and foremost, EJW for his persistence, encouragement, patience and wealth of knowledge, without whom this laboratory and project would be non-existent and my passion for stem cell research would never have blossomed into the life-changing experience it has become today; DO, for his patience, time, encouragement, captivating foreign accent and most of all for his strange, awkward but quick-witted humour, even during his transient naps in meetings and one-on-one conversations; NG, for his insistent encouragement that I should never hold back from asking for help to solve experimental problems out of my area of expertise, especially when it mattered most; NT and AB for their experience, patience and genuine care and concern for my well-being at all times of the day, in and out of the lab, and also their delicious cooking; CB for his mateship, lengthy technical, scientific and theoretical discussion of our respective projects, and resilience to my awful sense of humour; SKD for his knowledge, encouragement and experience and general good company, especially with the wine; DW, SD, SA, PF, SN, OH and JS for imparting all their knowledge and experience throughout my project and ensuring my happiness and well-being with jokes and encouraging comments at the hardest of times; and finally to GLB without whom the last few weeks of my project would have felt like the worst few weeks of my entire schooling, your company, encouragement, understanding and support made everything better.

Introduction

Alzheimer's disease (AD) is one of the most prevalent diseases of aging in the western world, affecting approximately one in three people over the age of 85 (Thies et al., 2013). In Australia, it has an estimated annual cost to the taxpayer of $4.9billion (Economics, 2011). Together with dementia, AD is the third leading cause of death in Australia (Statistics, 2012). A condition that presents strong links to Alzheimer's disease is Down's syndrome (DS). In DS patients, 100% will develop full-blown AD by 40 years of age (Zigman, 2013, Zigman et al., 1996), thus presenting itself as an effective model for study of AD.

Since their discovery, human pluripotent stem cells have been used as a model for a plethora of different diseases. More recently, human induced pluripotent stem cells (hiPSCs) have emerged as a novel platform for human disease modelling as they are patient-specific and recapitulate aspects of disease provided the desired cell type can be generated in vitro (Tiscornia et al., 2011, Park et al., 2008). hiPSCs have indeed been used to good effect to modelling a variety of diseases, including neurological disorders, and subsequent gene correction may also form the basis of cell based therapies (Yamanaka, 2007). hiPSCs are pluripotent cells that have the potential to differentiate into every cell type in the body (Yu et al., 2007), including various different neuronal and non-neuronal cell types following directed neuronal differentiation protocols (Briggs et al., 2013a, Briggs et al., 2013b, Chambers et al., 2009, Kim et al., 2010, Lancaster et al., 2013, Shi et al., 2012).

We have previously published the successful reprogramming of DS human induced pluripotent stem cells (hiPSCs) and their differentiation into forebrain neurons, thereby allowing us to study AD-related neuropathology *in vitro* (Briggs et al., 2013b). If we are to use such cultures to interrogate disease phenotypes, it is necessary to identify the exact type and abundance of the sub-types of neurons generated in culture. In addition to neurons, it has been shown that it is likely that glia, particularly astrocytes, play an important role in the

disease pathology of AD (Mrak and Griffinbc, 2001, Hu et al., 1998, Sukhatme et al., 1988, Itagaki et al., 1989). It was previously demonstrated that astrocytes can be successfully differentiated from hiPSCs (Emdad et al., 2012, Juopperi et al., 2012, Shaltouki et al., 2013), suggesting that disease-specific astrocytes could be produced to model early AD cellular phenotypes in the dish. Nevertheless, interrogating the role of neurons and astrocytes in an isolated manner can only go so far as to explaining disease pathogenesis in AD, thus a novel model system for elucidating how their interactions conspire to generate AD pathogenesis is necessary.

A potential method for quantification of cell-cell interaction is by employing a microfluidic culture platform (Taylor et al., 2005) (herein referred to as the 'interaction device'). This would allow simple and efficient quantification of the axonal growth of neurons. In addition to quantification of axonal growth, readouts such as transcriptional levels of disease- and neuronal development-associated genes in these cells could also help to identify AD-associated phenotypes when comparing DS and control neuronal and glial culture. In such an interaction device, the influence of cell-cell interactions can be quantified and compared for DS and control cells.

Our first aim was therefore to develop a novel astrocyte differentiation protocol that was both more rapid and more efficient than existing protocols. Parallel to this, we attempted to further characterise the neuronal subtypes that we generated *in vitro* with our established neural differentiation protocol. If successful, we would then use the knowledge gained from the control and DS neurons and astrocytes to predict and experimentally test whether co-culture of WT neurons or astrocytes with DS neurons or astrocytes could rescue the AD phenotype in their co-cultured DS counterpart cell-type. In the event that the proposed astrocyte differentiation protocol failed, we aimed to use magnetic activated cell sorting (MACS) to sort resident astrocytes from mature neuronal differentiation cultures, as we have

previously shown that these cells types are produced in small but substantial enough numbers for this purpose post day 45 when neuronal progenitors undergo a gliogenic switch (Briggs et al., 2013b). We hypothesised that, once in co-culture, the WT astrocytes would be able to partially, if not fully rescue the AD cellular phenotype in the DS neurons.

Although neurons and glia are both important co-constituent cells of the brain, the role of neurons as the main facilitators of learning and memory is in itself an inherently important research focus. Indeed, one of the most conspicuous features of AD is loss of memory retention. In the last decade it has emerged that methylation of DNA is an intrinsic contributing factor to development of the neuron (Wang et al., 2012, Aldinger et al., 2013). Most interestingly, it has been shown that the activity of some genes involved in genomic methylation, including DNMT1, DNMT3a and DNMT3b (as well as others), are also involved in transmitting and recording neuronal activity into epigenetic changes in the nucleus (Sharma et al., 2008, Miller and Sweatt, 2007), providing a potential mechanism for memory formation. Given that changes in DNA methyltransferase (DNMT) activity have been linked to depolarisation (Sharma et al., 2008, Yu et al., 2011), we hypothesised that depolarisation-generated neuronal activity plays an important role in learning, memory formation, and the functional development of human neurons.

During neuronal development, a number of different neurotransmitters can trigger depolarisation of cells (McCormick et al., 1993). The type of neurotransmitters that elicit a depolarising response vary with cell type (Strubing et al., 1995). Given that our differentiation protocol produces largely forebrain neurons that are presumably largely glutamatergic, investigation of how agents like glutamate affect the cells (Belhage et al., 1993) will help in understanding the role of depolarisation in neuronal development. Experimental cell non-specific depolarisation can be elicited through addition of KCl. A well-known response to depolarisation of neuronal cells is the upregulation of immediate

early genes (IEGs) during the first 3-4 hours (Sheng and Greenberg, 1990). To date, IEG responses to various neurotransmitters in human iPSC-derived cultured neurons has not been studied in depth.

It was previously demonstrated that in foetal mouse primary cortical neurons, depolarisation with KCl leads to a transient decrease in DNMT1 and DNMT3a mRNA expression (Sharma et al., 2008). Further to this, it has been shown that in adult mouse neurons, neuronal activity induces both demethylation and *de novo* DNA methylation (Guo et al., 2011). In mouse primary cultured neurons neuronal activity appears to cause a number of important changes in the DNA methylation of the neuronal genome through modulation of DNMT activity. Here we wished to test whether the same phenomenon occurs in cultured human iPSC-derived neurons. To do this, we investigated the effect of different depolarisation agents on DNMT3 expression in collaboration with Professor Ryan Lister, at UWA, who is currently determining activity-dependant DNA methylation changes in these same cells. We hypothesised that the mRNA expression of genes purportedly involved in maintenance and *de novo* DNA methylation, namely DNMT1, DNMT3a and DNMT3b, would be significantly altered in neurons following depolarisation. This would allow us to begin to tease out the exact mechanisms that influence how memory is laid down through activity-induced epigenetic changes.

Methods

Culture of hiPSCs

Work with these human-derived cells was performed with the informed consent of patients under the approval of Human Research Ethics Committee (HREC: 2008001651). Euploid lines (C79eu and C87eu) are isogenic controls of the Down's syndrome lines (C11DS and C18DS) in that they are all from the same individual and are genetically identical to their Down's syndrome counterparts, but they are not trisomic for HSA21. C11WT and C32WT cell lines are wild-type hiPSC clones from different individuals. All hiPSC lines (C11WT, C32WT, C79eu, C87eu, C11DS, C18DS) were maintained as manually-passaged bulk cultures on irradiated mouse embryonic fibroblast (MEF)-seeded 60x15mm organ culture dishes (BD) in Dulbecco's modified Eagle's medium (DMEM)/F12 culture medium supplemented with 20% knockout serum replacement (KOSR), 1X nonessential amino acids, 1X GlutaMAX, along with 0.1 mM β-mercaptoethanol and 100ng/mL of human basic fibroblast growth factor (bFGF) (all from Invitrogen).

Cell cycle analysis of DS and control lines

All hiPSC lines (C11WT, C32WT, C79eu, C87eu, C11DS, C18DS) were manually passaged from feeder-dependant organ culture dishes onto ECM-coated (Sigma) six-well plates and cultured in MEF-conditioned medium supplemented with 0.1 mM β-mercaptoethanol, 100ng/mL bFGF (both from Invitrogen) for 8 days. At day 8, EdU was added according to the kit's protocol and left to incubate for 2 hours. EdU of DS and control lines was carried out using the Click-iT EdU Flow Cytometry Assay Kit (Invitrogen) using the 488nm secondary fluorescent probe, according to the manufacturer's protocol. FACS was processed on a LSR II analysing flow cytometer (BD). EdU data was analysed using FCS Express software package (DeNovo Software).

Neuronal differentiation of hiPSCs (excluding those used for depolarisation)

The neuronal differentiation protocol was largely based on that by Briggs et al. (Briggs et al., 2013b) with some modifications. For differentiation, cells were manually passaged from feeder-dependant organ culture dishes onto ECM-coated (Sigma) six-well plates and cultured in MEF-conditioned medium (Dulbecco's modified Eagle's medium (DMEM)/F12 culture medium supplemented with 20% knockout serum replacement (KOSR), 1X nonessential amino acids, 1X GlutaMAX (all from Gibco) that has been collected and filtered (0.22μm) after 24hrs on irradiated MEFs in the first 7 days of culture) supplemented with 0.1 mM β-mercaptoethanol, 100ng/mL bFGF (both from Invitrogen). All hiPSC lines were cultured for at least 7 days post manual passaging (sometimes up to 14 days in DS lines) until wells were between 50 and 70% confluent with cell colonies. These were changed directly into DMEM/F12 with 20% KOSR, 1X nonessential amino acids and 1X GlutaMAX, supplemented with 10 μM SB431542 (Sigma) and 5 μM dorsomorphin (Stemgent) for the first 6 and 12 days of differentiation, respectively. This media was changed every two days, with a progressively larger component of N2B27 medium each change (while still maintaining concentration of small molecules) so that N2B27 made up 25%, 50%, 75% and 100% of the medium on days 4, 6, 8 and 10, respectively.

On day 6, neuronal EBs (referred to herein as neurospheres) were formed by 5 minutes incubation in 1 mg/ml dispase (Gibco) at 37°C, rinsing well twice with N2B27, before using one smooth, uninterrupted, uniform scrape across the bottom of the well with a cells scraper in order to lift up cell colonies in as intact a state as possible (the more intact the colonies are, the better the formation of neurospheres). A 5mL pipette was then used to transfer cells to a 15 mL falcon tube to minimise shear stress on the in-tact colonies now in suspension. After cells settled in bottom of tube, N2B27 rinse media was replaced day 6

differentiation media and cells were transferred (again with a 5mL pipette) and seeded into Ultra-low Cluster plates (Costar Corning Sigma) in which the suspended colonies slowly formed neurospheres, progressively aggregating over the following six days.

On day 12, neurospheres were transferred using a P1000 pipette onto ECM-coated (Sigma) six-well plates. N2B27 media was then changed every 3–4 days and, from day 45 post-induction, cells were matured by the addition of 20ng/mL BDNF, 20ng/mL GDNF (R&D), 200nM ascorbic acid, and 0.5mM dibutyryl-cAMP (Sigma) until day 60. Adherent cultures were then passaged every 14 to 21 days, by 2 – 3 min incubation in StemPro Accutase (Life Technologies) at a 1:3–1:6 ratio, eventually leading to the almost complete dissociation of persisting neurosphere aggregates.

Astrocyte differentiation

The astrocyte differentiation protocol is largely adapted from the recent protocol by Shaltouki et al. (Shaltouki et al., 2013) but with unique modifications largely influenced by findings noted from our neuronal differentiation protocol (Briggs et al., 2013b). Wild-type hiPSC lines C11 and C32 were grown for five to seven days post manual passaging into ECM-coated (Sigma) six-well plates. They were then be subjected to six days of the neuronal differentiation protocol (Briggs et al., 2013b). At day six, neural progenitors were passaged onto fresh ECM-coated (Sigma) six-well plates and transitioned to Neurobasal medium (Gibco) supplemented with EGF (10ng/mL), human LIF (100U/mL) (Millipore) and 1X GlutaMAX (Gibco) for expansion, changing media every three to four days and passaging every 7 to 10 days, but now with TrypLE (Gibco) (3-5 min incubation). At week 4, these were to be passaged again and transitioned to Neurobasal medium supplemented with CNTF (5ng/mL), BMP-7 (10ng/mL) and bFGF (10ng/ml) in the presence of 1% FBS, changing

media every 3 to 4 days and passaging every 7 to 10 days until maturity (or indefinitely if desired).

Immunocytochemistry

Differentiated cultures were analysed using standard immunocytochemistry (ICC) analysis methods. Cells were seeded onto ECM-coated (Sigma) glass coverslips then grown in relevant conditions for desired length of time before fixation. Cells were rinsed with two 5-minute washes in PBS+/+ before 20-minute incubation in 4% PFA at RT to fix cells. Cells were then rinsed again with two 5-minute washes in PBS+/+ and (if appropriate for primary antibody) cells were permeablised with 0.1% Triton-X100 in PBS+/+ for 15 minutes at room temperature. Cells were then rinsed with two 5-minute washes in PBS+/+ before being blocked with blocking buffer (10% goat serum and 0.05% Triton-X100 in PBS-/-) for 30 minutes at RT. Before incubation with primary antibody, cell were rinsed with two 5-minute washes in PBS+/+. Primary antibody incubation in incubation buffer (10% blocking buffer in PBS-/-) was performed overnight (~12 hours) at 4°C. The following antibodies were used: A2B5 (1:500; Millipore, MAB312), BIIItub (1:1000; Millipore, MAB1637), GABA Aα1 (1:500; Millipore, 06-868), Gephyrin (Synaptic Systems, 147 011), GFAP (1:1000; dako, Z033429-2), NeuN (1:1000; Millipore, #ABN78), Pax6 (1:1000; Covance, [Rb, polyclonal]), PSD95 (1:500; Synaptic Systems, 124 011), S100β (1:1000; Sigma, s2532), SV2 (1:500; DSHB), synapsin-1 (1:500; EMD Millipore, 574777), synaptophysin (1:500; Cell Signalling, 5461). Cells were then rinsed with two 5-minute washes in PBS+/+ before applying secondary antibody in incubation buffer for 2hrs at RT. Both secondary antibodies were applied in a 1:1000 dilution: Alexa Fluor 488nm Goat Anti-Mouse IgG (Invitrogen, A11001) and Alexa Fluor 568nm Donkey Anti-Rabbit IgG (Invitrogen, A10042). Finally, coverslips were rinsed with two 5-minute washes in PBS+/+ before being mounted on glass slides with

ProLong Gold Antifade Reagent with DAPI (Life Technologies) and sealed with quick-dry clear nail polish (Cutex 'Quick 'n' Go').

A2B5 Magnetic Activated Cell Sorting of Glial-like Neuronal Differentiated Cells

In the event that astrocytes could not be produced for co-culture of neurons, magnetic activated cell sorting (MACS) was proposed as an alternative. 150 day-old glia-like neuronally differentiated C11 hiPSC cultures were harvested using TrypLE (Gibco). Cells were sorted using the Anti-A2B5 MicroBead Kit (Miltenyi Biotec) according to the manufacturer's protocol. Cells were counted post-sort, and negative, positive and unsorted samples were each plated onto coverslips at the same density of ~30,000 cells/cm^2 for analysis by immunocytochemistry.

Neuronal Differentiation for Depolarisation Experiment

The neuronal differentiation protocol was largely based on three previously established protocols, with some modifications (Briggs et al., 2013b, Chambers et al., 2009, Kim et al., 2010). For differentiation, wild-type hiPSC lines, C11 and C32, were manually passaged from feeder-dependant organ culture dishes onto ECM-coated (Sigma) six-well plates and cultured in MEF-conditioned medium supplemented with 0.1 mM β-mercaptoethanol, 100ng/mL bFGF (both from Invitrogen) for 8 days until wells were between approximately 60 - 70% confluent with cell colonies. These were changed directly into DMEM/F12 with 20% KOSR, 1X nonessential amino acids and 1X GlutaMAX, supplemented with 10 µM SB431542 (Sigma) and 5 µM dorsomorphin (Stemgent) for the first 6 and 12 days of differentiation, respectively. This media was changed every two days, with a progressively larger component of N2B27 medium each change (while still maintaining concentration of

small molecules) so that N2B27 made up 25%, 50%, 75% and 100% of the medium on days 4, 6, 8 and 10, respectively.

On day 6, neuronal EBs (referred to herein as neurospheres) were formed by 5 minutes incubation in 1 mg/ml dispase (Gibco) at 37°C, rinsing well twice with N2B27, before using one smooth, uninterrupted, uniform scrape across the bottom of the well with a cells scraper in order to lift up cell colonies in as intact a state as possible (the more intact the colonies are, the better the formation of neurospheres). A 5mL pipette (Sigma Corning Costar) was then used to transfer cells to a 15 mL falcon tube (BD) to minimise shear stress on the in-tact colonies now in suspension. After cells settled in bottom of tube, N2B27 rinse media was replaced day 6 differentiation media and cells were transferred (again with a 5mL pipette) and seeded into Ultra-low Cluster plates (Costar Corning Sigma) in which the suspended colonies slowly formed neurospheres, progressively aggregating more and more throughout the time in suspension culture. Neurospheres were subsequently expanded in Ultra-low Cluster plates until 60 days post induction.

From day 12, N2B27 media was then changed every 3–4 days and, from day 45 post-induction, cells were matured by the addition of 20ng/mL BDNF, 20ng/mL GDNF (R&D), 200nM ascorbic acid, and 0.5mM dibutyryl-cAMP (Sigma) until day 60. On day 60, neurospheres were broken up into smaller neurospheres using a P1000 pipette before being seeded onto ECM-coated (Sigma) six-well plates. Adherent cultures were passaged 4 times, approximately every 20 days, by 2 – 3 min incubation in StemPro Accutase (Life Technologies) at a 1:3–1:6 ratio, leading to the almost complete dissociation of most neurosphere aggregates. After passage 4, cells were left to mature in culture, continuing to be maintained on N2B27, until day 164 post induction when depolarisation began.

Immediate Early Gene Expression Analysis

Before the depolarisation experiment could begin, the neurons used for depolarisation had to first be shown to be of a maturity in which they were depolarisable. This was to be done using analysis of IEG expression 3 hours post stimulation with the respective depolarisation solutions. Cells were depolarised by addition of 567uL of relevant depolarisation solution (detailed in the Table 1) per 1mL of N2B27 media, with a control of 50ul of PBS+/+ (Gibco). At three hours post depolarisation, cells were harvested for RNA Extraction, converted to cDNA and run in triplicate on qPCR for upregulation of IEGs.

Table 1 | Formulation of depolarisation solutions used for treatment of day 164 neurons. Salt concentrations calculated so that when added to media, the overall molarity remains the same so as to avoid hypertonic shock of the cells.

Component (mM in ddH_2O)	IsoCtrl	IsoGlut	IsoKCl
HEPES	10.9	10.9	10.9
CaCl	1.8	1.8	1.8
MgCl	0.8	0.8	0.8
$NaHCO_3$	26.2	26.2	-
NaCl	51.7	51.7	-
$NaH_2PO_4 \cdot H_2O$	0.9	0.9	-
KCl	5.33	5.33	136 (final conc. in media = 50mM)
Glutamate	-	2.76 (so final conc. in media = 1mM)	-

Depolarisation of Late Neuronal Cultures

The depolarisation protocol was developed with reference to previously published experiments in the literature (Sharma et al., 2008). On day 163 post neuronal induction, all cells lines were changed with fresh N2B27 (the day before the experiment begun). 2mL of media was used on each well of a six-well plate (Sigma Corning Costar). C32 hiPSC-derived neuronal cells were harvested at four time points, 0, 24, 48 and 72 hours post depolarisation, where cells were depolarised at 0 hours, and returned to normal N2B27 media at 24 hours. The experiment was performed in quadruplicate (only differing in time since final passage to allow for sufficient morphological and cell physiological maturation in culture: cells were from 62 days, 61 days, 41 days and 39 days post final passage) to account for differences in morphological and cell physiological maturation of neurons post passage. Therefore, for each time point, every temporally differentially passaged set of wells was treated with each of the depolarisation solutions, yielding 48 unique samples across the 4 time points (3 depolarisation conditions x 4 temporally different passages x 4 time points = 48 unique treatments, as shown in Table 2). Cells were depolarised by addition of 567uL of relevant depolarisation solution (detailed in Table 1) per 1mL of N2B27 media.

Table 2 | Tabulated illustration of the treatment at each time point (isoCtrl, isoKCl & isoGlut) for each set of plates. The sets were of plates that, at depolarisation, only differed in the period of time since p4.

Time point	62 days	61 days	41 days	39 days
0 hours	isoCtrl, isoKCl & isoGlut	isoCtrl, isoKCl & isoGlut	isoCtrl, isoKCl & isoGlut	isoCtrl, isoKCl & isoGlut
+24 hours	isoCtrl, isoKCl & isoGlut	isoCtrl, isoKCl & isoGlut	isoCtrl, isoKCl & isoGlut	isoCtrl, isoKCl & isoGlut
+48 hours	isoCtrl, isoKCl & isoGlut	isoCtrl, isoKCl & isoGlut	isoCtrl, isoKCl & isoGlut	isoCtrl, isoKCl & isoGlut
+72 hours	isoCtrl, isoKCl & isoGlut	isoCtrl, isoKCl & isoGlut	isoCtrl, isoKCl & isoGlut	isoCtrl, isoKCl & isoGlut

RNA Extraction

All RNA extractions were performed using the NucleoSpin RNA II (Macherey-Nagel) RNA isolation kit according to the manufacturer's protocol. The following (shown in Table 3) are the yields gained for each extracted sample, accompanied by the spectral purity ratios:

Table 3 | Information on RNA yield post RNA extraction of initial samples from IEG upregulation trial post 3 hours of neuronal depolarisation. This includes the purity ratios calculated from the spectral reading of the samples.

Sample	Yield (ng/µl)	260nm/280nm	260nm/230nm
PBS ctrl1	82.4	2.08	1.74
PBS ctrl2	104.88	2.08	2.01
PBS ctrl3	154.18	2.09	1.24
isoCtrl1	112.11	2.09	0.75
isoCtrl2	113.56	2.08	1.5
isoCtrl3	140.72	2.07	1.33
isoKCl1	120.73	2.06	1.65
isoKCl2	132.70	2.11	0.76
isoKCl3	178.45	2.07	0.89
isoGlut1	145.6	2.11	1.90
isoGlut2	136.95	2.08	2.08
isoGlut3	187.5	2.07	2.08

Synthesis of cDNA

All cDNA synthesis was performed using the iScript cDNA synthesis kit (Bio-Rad) according to the manufacturer's protocol.

Quantitative Real Time Polymerase Chain Reaction

All qPCR reactions were performed using the SsoFast EvaGreen Supermix (Bio-Rad) according to the manufacturer's protocol. Here follow the sequences for all primers used in this project listed by gene name in alphabetical order from 5' to 3':

ARC for:	GCGGCTCTGAGGAGTACTGGCT
ARC rev:	ATGGCCTCTCGGGACAGCGT
BDNFExIV for:	CTCCGCCATGCAATTTCCAC
BDNFExIV rev:	GCCTTCATGCAACCAAAGTA
cFOS for:	CCGGAGGAGGGAGCTGACTGA
cFOS rev:	GGATCTTGCAGGCAGGTCGGTG
DNMT1 for:	CCTAGTTCCGTGGCTACGAGGAGAA
DNMT1 rev:	TCTCTCTCCTCTGCAGCCGACTCA
DNMT3a for:	GTCCTGCAGGTGGCCAGCAG
DNMT3a rev:	CCTCCACGGCCTTGGCAGTG
DNMT3b for:	GAAAGCTAGGGTGCGAGCTGGC
DNMT3b rev:	ACTGGTTGCGTGTTGTTGGGTT
EGR1 for:	AGCCCTACGAGCACCTGA
EGR1 rev:	GGCAGTCGAGTGGTTTGG
Neuritin for:	AGCATGGCCAACTACCCGCA
Neuritin rev:	CGTAAGGGCTGTGACCGTGCAG
PLAT for:	TCTTACCAAGGTTGCAGCGAGCCA
PLAT rev:	TGGTCCTCGTAGCACGTGGCC

Interaction Device Culture

Devices were manufactured by Dr Nick Glass (Tissue Engineering and Microfluidics Group, Australian Institute of Bioengineering and Nanotechnology, The University of Queensland, St Lucia, 4072, QLD, Australia) according to the previously described protocol (Taylor et al., 2005). Device was set-up by placing a fresh, hydrophilic device on a glass coverslip. Neurons were differentiated to an appropriate day post-induction to ensure maturing neuronal morphology (all neurons were taken from day 100+ post neuronal induction). Neurons were then passaged by 2 – 3 minute incubation in StemPro Accutase (Life Technologies) and

seeded into the device at ~30,000 cells/cm^2. Device was left overnight in incubator for cells to settle and adhere. Media was topped up daily with 100 – 200µl media per well to ensure device did not dry out, and change every 3 to 4 days to avoid over-concentration of cell paracrine and metabolic excrement.

Results

Cell Cycle Analysis of DS and Control Lines

Upon culture of the WT, euploid and DS hiPSC lines, I observed that the DS cell lines grew more slowly than control lines. To assess and compare the proliferation of the DS and control cell lines, an EdU incorporation assay was performed to compare cell cycle state of the six cell lines. As shown in figure 1, all lines are similar in their apparent rate of proliferation as measured by incorporation of EdU over a two hour period. However, it appears that there may be a trend showing that there are more cells in G_1/G_0 for the euploid lines than in the other four. It should be pointed out though, that there were no replicates preformed, so I was unable to establish whether there was a significant difference between DS (C11DS and c18DS) and control lines (euploid control: C79eu, C87eu; wild-type: C11WT, C32WT).

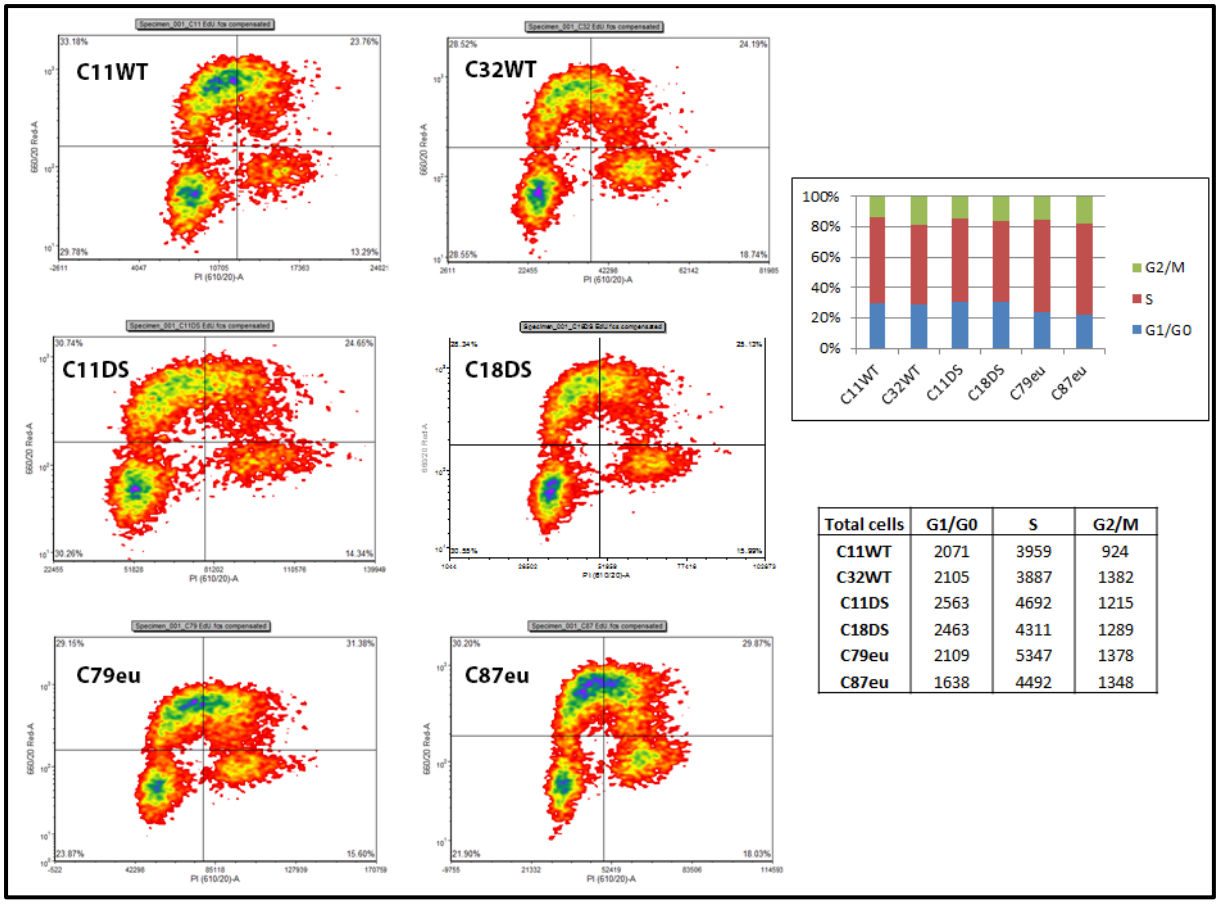

Total cells	G1/G0	S	G2/M
C11WT	2071	3959	924
C32WT	2105	3887	1382
C11DS	2563	4692	1215
C18DS	2463	4311	1289
C79eu	2109	5347	1378
C87eu	1638	4492	1348

Figure 1 | Cell cycle state analysis of all six hiPSC lines with cells stained using a 2-hour incubation with EdU. To the left, the six scatter plots show density distribution of fluorescence activated cell sorting for EdU compared to PI for the six cell lines. On the right, the top graph shows the proportion of cells in each part of the cell cycle for each of the six cell lines; the table below shows the exact number of cells in each part of the cell cycle. These were the numbers used to generate the graph above.

Characterisation of hiPSC-derived Neuronal Differentiation with ICC

The identity and composition of hiPSC-derived neuronal cultures was characterised with ICC staining at two stages post induction (day 127 and day 156). Before staining, bright field photos of the unfixed cells were captured while still in culture to assess morphology of the cells and the neuronal networks formed (see figure 2). I observed that the morphology of

individual cells was neuronal and that these cells formed extensive neuronal networks across the culture with bundled axonal connections between adherent neurospheres and smaller groups of neurons.

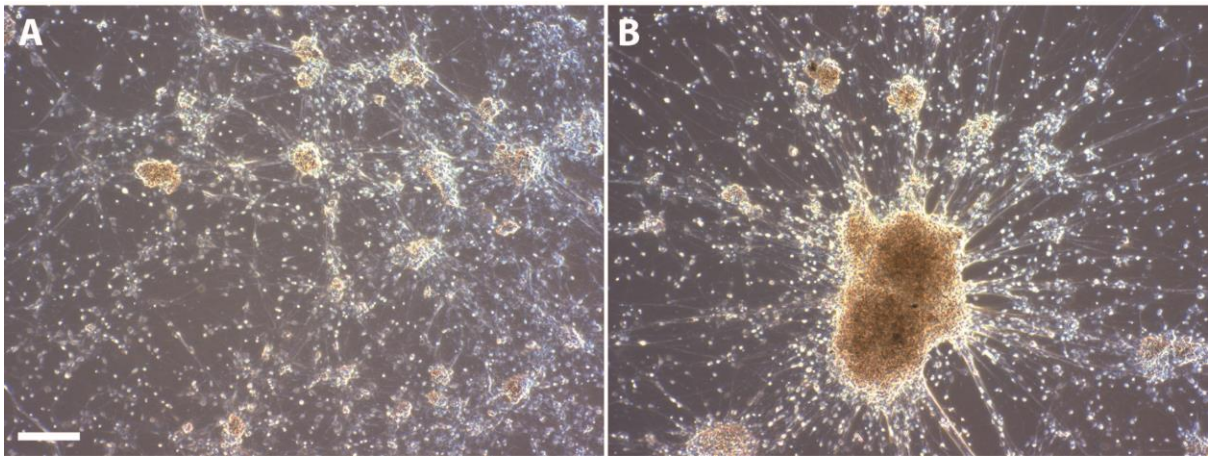

Figure 2 | Bright field photos of maturing C32WT neurons (day 156) before ICC (scale bar = 50µm). Neuronal morphology of the cells is distinct, and persistent neurospheres are still present in culture.

Next the expression of key neuronal markers was investigated. At day 127 cells were generally positive for Map2 and βIIItubulin (approximately >90% for each) and $NeuN^+$ cells made up a very small proportion of cells in culture (approximately <5%), mostly occurring in persistent neurospheres (the larger the adherent neurosphere, the greater the proportion of $NeuN^+$ cells contained within).

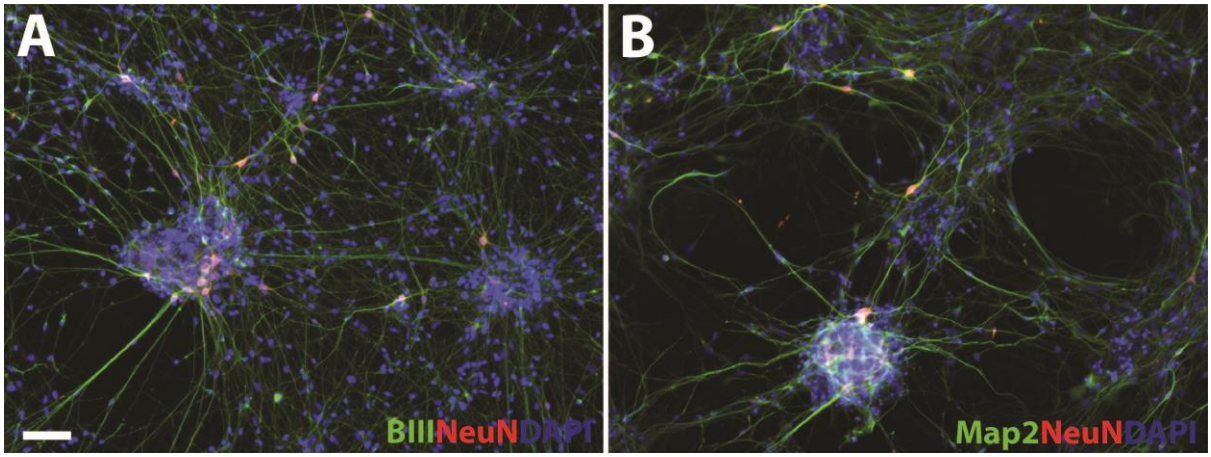

Figure 3 | Immunocytochemistry of day 127 of C32WT neuronal differentiation (scale bar = 50µm). A shows presence of NeuN$^+$ progenitors, with extensive BIII tubulin staining throughout the neurons in culture. B shows that cells are also Map2$^+$ containing a similar proportion of NeuN$^+$ progenitors in neurospheres in culture.

At day 156, a more extensive array of markers was used to characterise the more mature cells. The cell-type-specific markers βIIItubulin and GFAP were used in conjunction with Pax6, s100β and A2B5. The vast majority of cells show presence of βIIItubulin, but were negative for Pax6, indicating these cells were mainly mature neurons, and the cultures no longer contained early progenitors (figure 4A). There was also a number of glia present (estimated at around 10%), indicated by the expression of GFAP in contrast to BIII tubulin (figure 4B) and the presence of s100β$^+$ cells (~15-20%). Interestingly s100β only partly co-localised with GFAP$^+$ cells (figure 4C) although both are thought to be glial markers. There also appeared to be expression of the oligodendrocyte precursor- and astrocyte-marker A2B5 in a small number of cells (figure 4D).

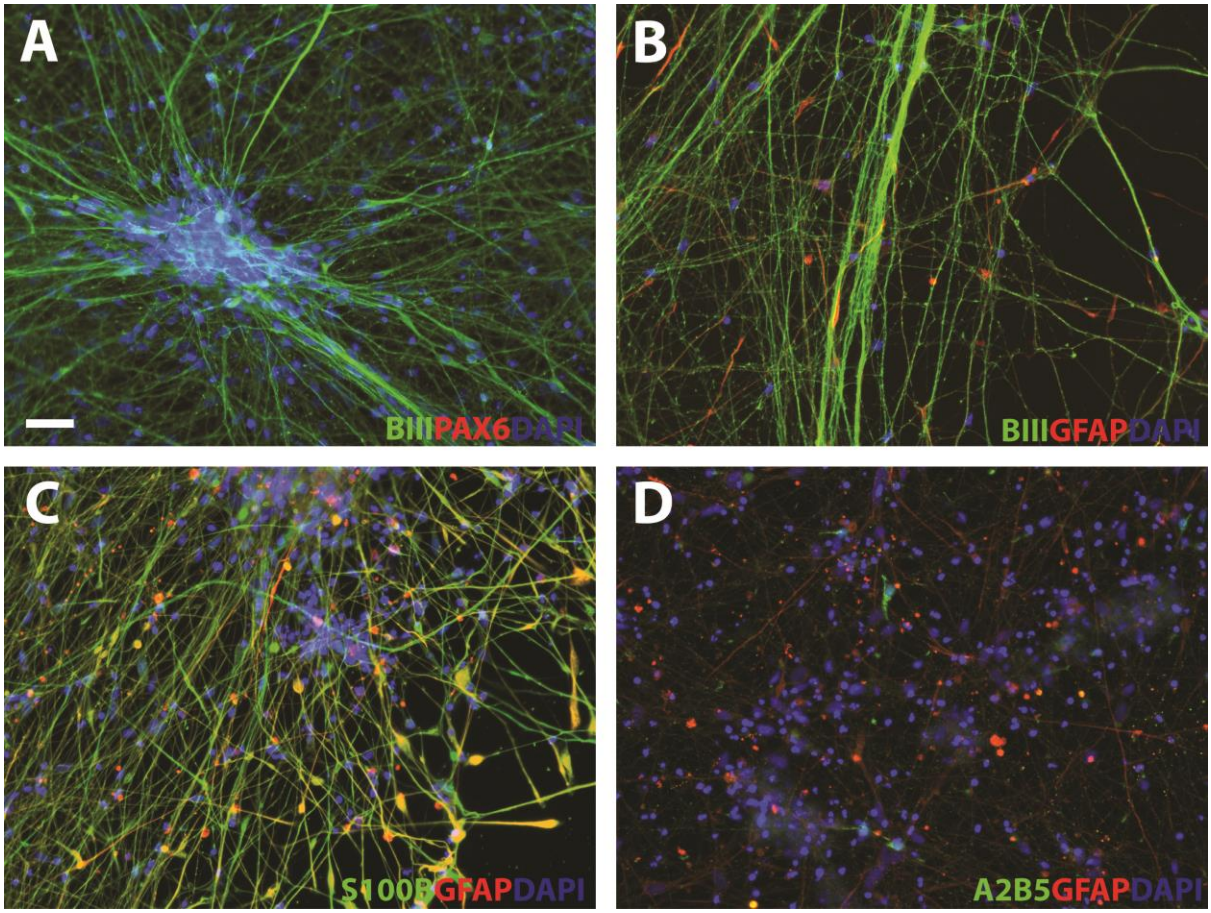

Figure 4 | Immunocytochemistry of day 156 of C11WT and C32WT neuronal differentiation (scale bar = 50µm). A shows no presence of Pax6 progenitors, but extensive βIIItubulin staining throughout the neurons in culture. B shows that βIIItubulin$^+$ neurons are distinct from GFAP$^+$ glia in culture. C shows that there are a large proportion of S100β$^+$ cells in culture, a substantial proportion of which are GFAP$^+$ as well. Finally, D shows that although they are not double positive for GFAP, there are a small number of A2B5$^+$ cells in culture. For control ICC stains see appendices, figure A1.

The immunofluorescence analyses of the same day 156 neurons (see figure 5) revealed the presence of synaptic markers synapsin-1, PSD95, and SV2 indicating that cultures had

extensive synaptic connections. There was also presence of gephyrin^{+} cells detected in the population, indicating GABAergic or glycinergic inhibitory neuronal identity. These gephyrin^{+} cells were distinct from populations of NeuN^{+} late neuronal progenitor/early neuronal cells, suggesting that these cells had passed through a post-NeuN^{+} stage of neuronal maturation to become gephyrin^{+}. There appeared to be some GABA Aα1, but no conclusive GAD65/67 staining could be detected. However, this may have been due to the fact the antibodies were becoming less efficient due to time since production. Without positive controls (see appendices, figure A1), we were unable to accurately assess the quality of these antibodies.

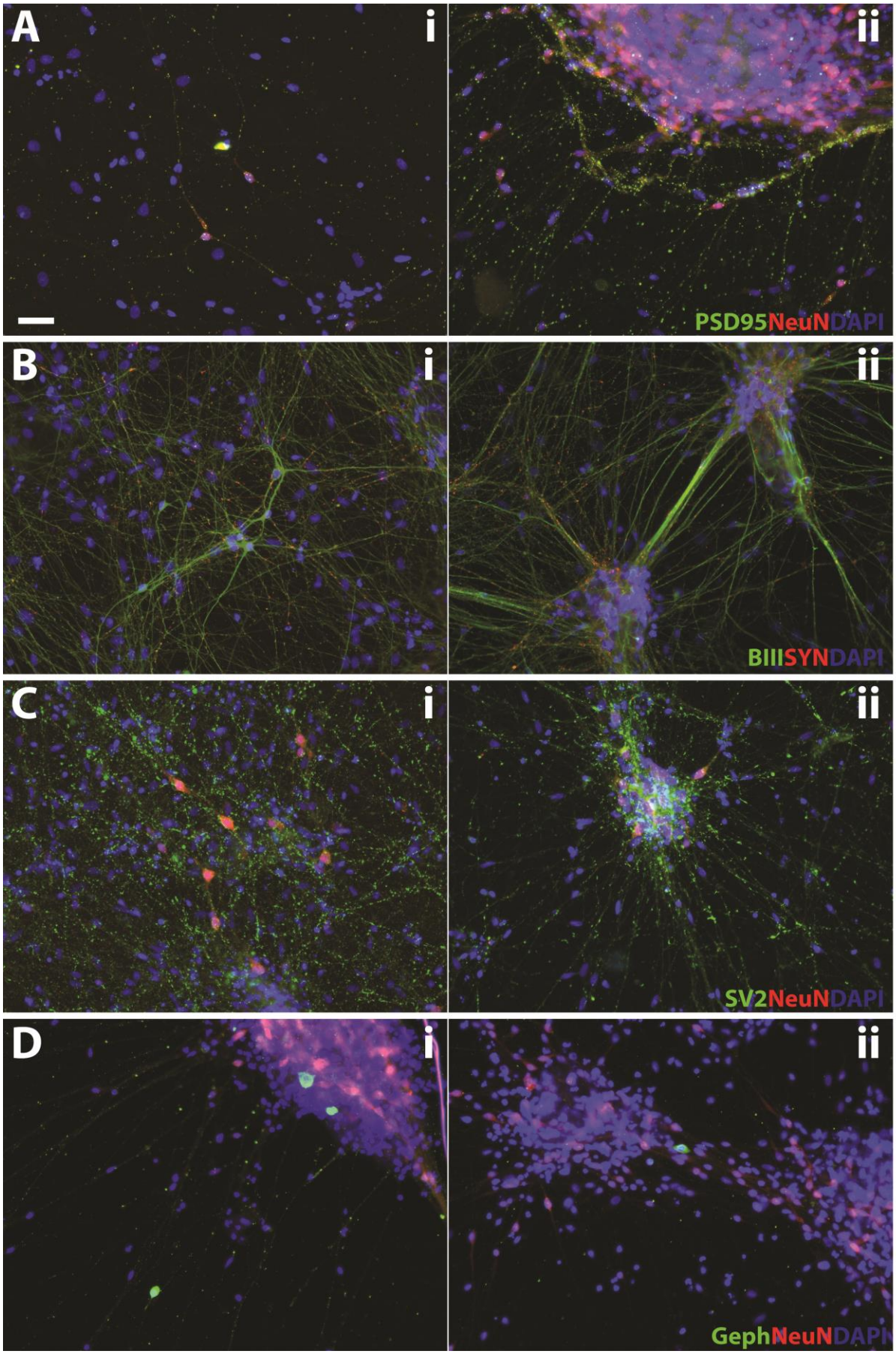
A
i
ii
PSD95NeuNDAPI
B
i
ii
BIIISYNDAPI
C
i
ii
SV2NeuNDAPI
D
i
ii
GephNeuNDAPI

Figure 5 | Immunofluorescence images of ICC of C11WT and C32WT neuronal differentiation (day 156) for synaptic markers PSD95, synapsin-1 and SV2, as well as for the inhibitory interneuron marker gephyrin (scale bar = 50µm). Aii shows extensive PSD95 punctate staining indicating the presence of maturing synapses, Ai supports this by showing that the PSD95^{+} synapses are also present on both NeuN^{+} and NeuN^{-} cells, even away from persistent neurospheres in culture. Bi and ii show staining of synapsin-1+ synapses, marking synaptogenesis. Ci shows prolific inhibitory pre-synapse marking by SV2, on both NeuN^{+} and NeuN^{-} cells, while Cii shows that this is concentrated near neurospheres. Di and ii show that there are a small number of gephyrin positive cells. As expected, these are distinct from NeuN^{+} early neuronal progenitors. For control ICC stains see appendices, figure A1.

Development of Novel Astrocyte Differentiation Protocol

To foster astrocyte differentiation, we first attempted to culture C11WT and C32WT cells into suspension on Ultra-low Cluster plates (Costar Corning Sigma) for days 6 to 12 of the differentiation protocol (as with the neuronal differentiation protocol), and then seed the patterned cells in Neurobasal supplemented only with EGF (10ng/mL), human LIF (100U/mL) (Millipore) and 1X GlutaMAX (Gibco). At this time however, the neurospheres would not form and cells began to disintegrate and form a uniform thin film of cell matter. It was thus impossible to acquire images of the cells.

On the second attempt, the cells were plated onto ECM on day 6, via passage with dispase (1mg/ml for 5 mins), instead of being placed in suspension on ultra-low attachment plates; however, this resulted in apoptotic morphology and mass cell death. This time, the efficiency of the ECM attachment coating of the culture dishes was questionable. The

protocol was therefore attempted a third time. The results were similar, however and few cells persisted beyond day 6. Despite the inefficiency of differentiation and the large amount of cell death, we did obtain low numbers of cells with astrocyte precursor-like morphology (figure 6A). We therefore decided to assess which passage medium would be most suitable for these cells after day 6. We trialled two passaging methods, dispase (1mg/ml for 5 mins) and TrypLE (5 mins), and assessed whether this could help foster expansion of the cells (see figure 6A). The passaging of the astrocytes was however not ideal. Photos were taken of the cells (see figure 6B and 6C) and the plate was discarded.

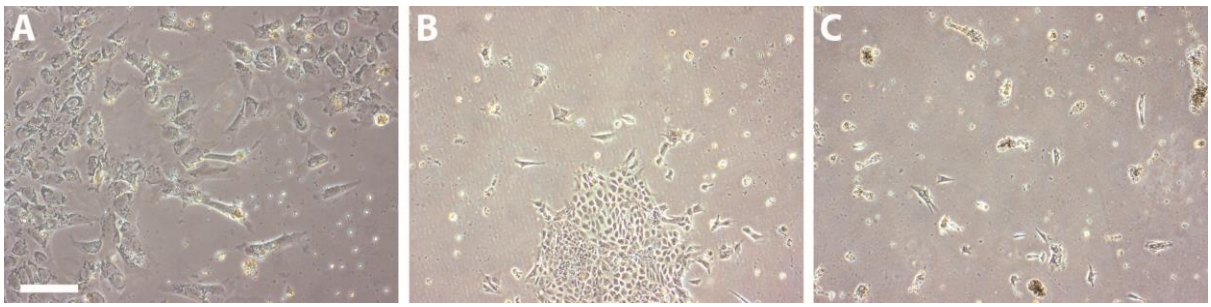

Figure 6 | Bright field of C32 astrocyte differentiation (Scale bar = 50µm). A shows cells at day 8 post induction, before passaging. B and C are cells post-passage (with dispase and TrypLE, respectively). In B, the majority of cells did not survive, the cells that remained, however, can be seen to be in clusters, as shown, with neuronal- or glial progenitor-like morphology. In C, the morphology can be seen to be much as it is in B, however the TrypLE completely dissociates the cells and so there were no clumps or cluster as there were in the dispase-passaged well.

Given the repeated failure, I decided to modify the cytokine cocktail that induces astrocyte differentiation from hiPSCs and titrate the cytokines EGF and LIF. The constitution of the media that corresponds to the pictures is shown in table 4. Two different substrates were

trialled at this time as well (Collagen I (Life Technologies), figure 7; ECM (sigma), figure 8), however this still resulted in similar results to the second and third attempts with a large amount of cell death, eventually leading to complete cell death a short number of days after these photos were taken. The protocol therefore had to be modified yet again to determine what protocol could yield efficient astrocyte differentiation.

Titrations	Human LIF		
EGF	**10U/mL**	**100U/mL**	**1000U/mL**
1ug/mL	A	B, C	D
10ug/mL	E	F, G	H
50ug/mL	I	J, K	L

Table 4 | Concentrations of cytokines used for the corresponding pictures in the following two figures. EGF and LIF were the two cytokines titrated out for two surface coatings, Collagen I (figure 7) and ECM (figure 8).

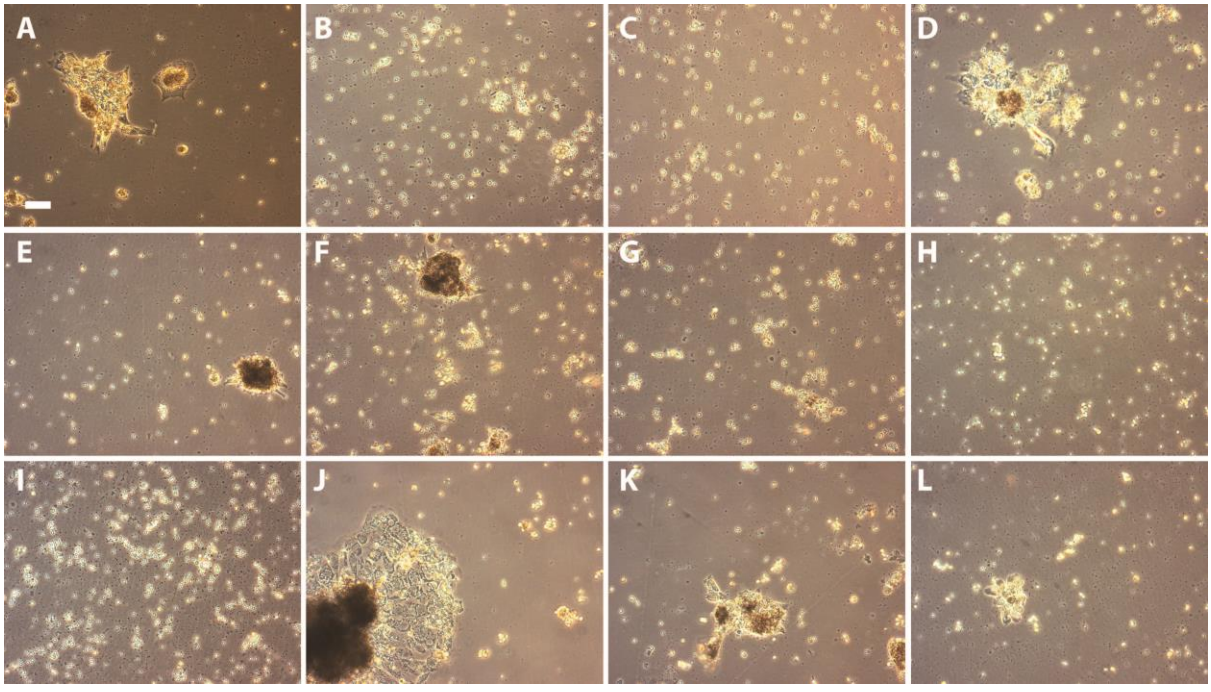

Figure 7 | Bright field images of C11 astrocyte differentiation trial on Collagen I (see table 4 for concentrations corresponding to pictures) (scale bar = 50µm). Very few wells

maintained basic cell morphology in infrequent and remote parts of the wells, but any of this that was found was lost in a matter of days after these pictures were taken.

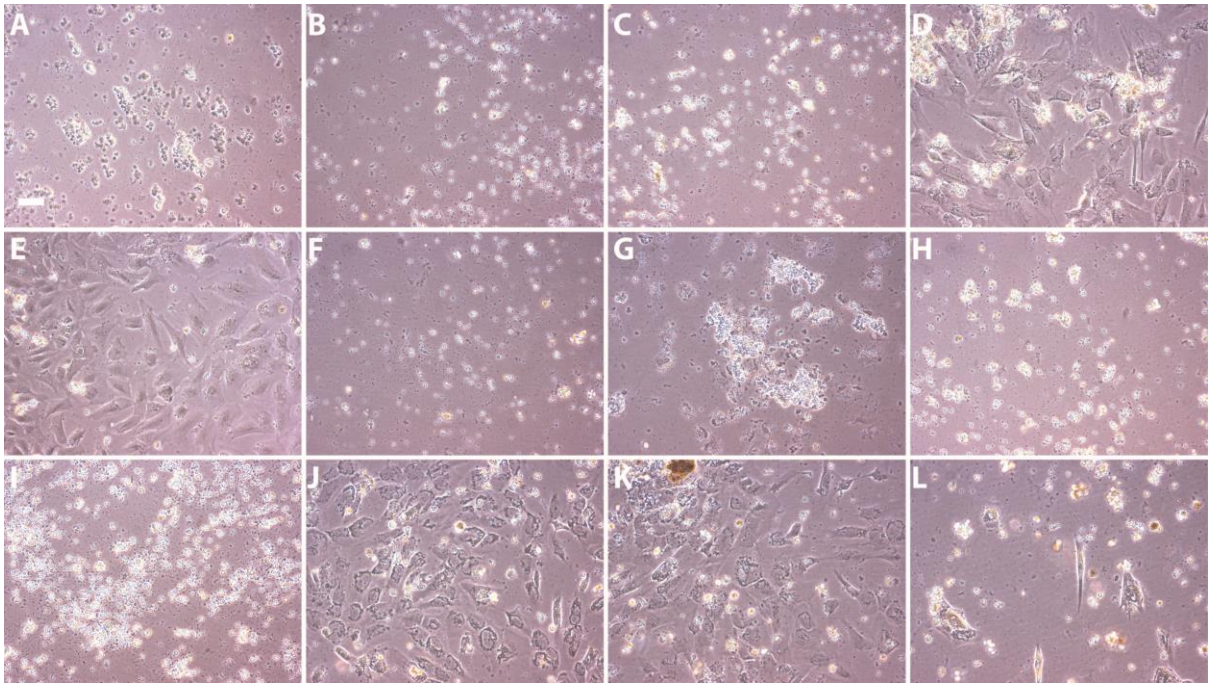

Figure 8 | Bright field images of C11 astrocyte differentiation trial on ECM (see table 4 for concentrations corresponding to pictures) (scale bar = 50µm). The ECM initially appear to promote survival better than Collagen I, with some wells maintaining basic cell morphology – albeit in infrequent and remote parts of the wells – but any of this morphology that was found was lost in a matter of days after these picture were taken.

On the fifth attempt, I intended to leave cells until day 18 of the neuronal differentiation protocol before adding cytokines (to ensure full neuroepithelial fate conversion) however, cells were still not displaying the desired astrocyte morphology and exhibited large amounts of cell death. At this point, due to the time constraints of the project, there was no longer time to continue trialling protocols for differentiation of astrocytes. We concluded that our

adaptation to published astrocyte differentiation protocols was suboptimal and that neural progenitors fail to undergo a gliogenic switch imposed by the exogenous growth factors used in this project.

Neuronal Differentiation of DS Cell Lines

In order to minimise variability amongst cell lines, careful maintenance of hiPSC lines was required to ensure that differentiation could be induced at the same time in all six lines. Throughout the project, growth of C11WT and C32WT cultures was able to be facilitated more frequently and with less difficulty than DS cultures and thus differentiation of these two WT lines was successfully completed independently of the coordinated DS and control differentiation (see figures 2, 3, 4 and 5). Consequently, simultaneous neuronal induction of all six lines was only able to be accurately coordinated once during this project (this was the same round of passaged cells used for EdU analysis). Cells appeared to progress normally through differentiation from days 0 to 11, however, when the cells reached day 12 and were plated down on ECM-coated plates, there was massive cell death and the cultures did not appear neuronal (see figure 9). Reasons for this failure are unclear, though a number of possibilities are proposed in the discussion.

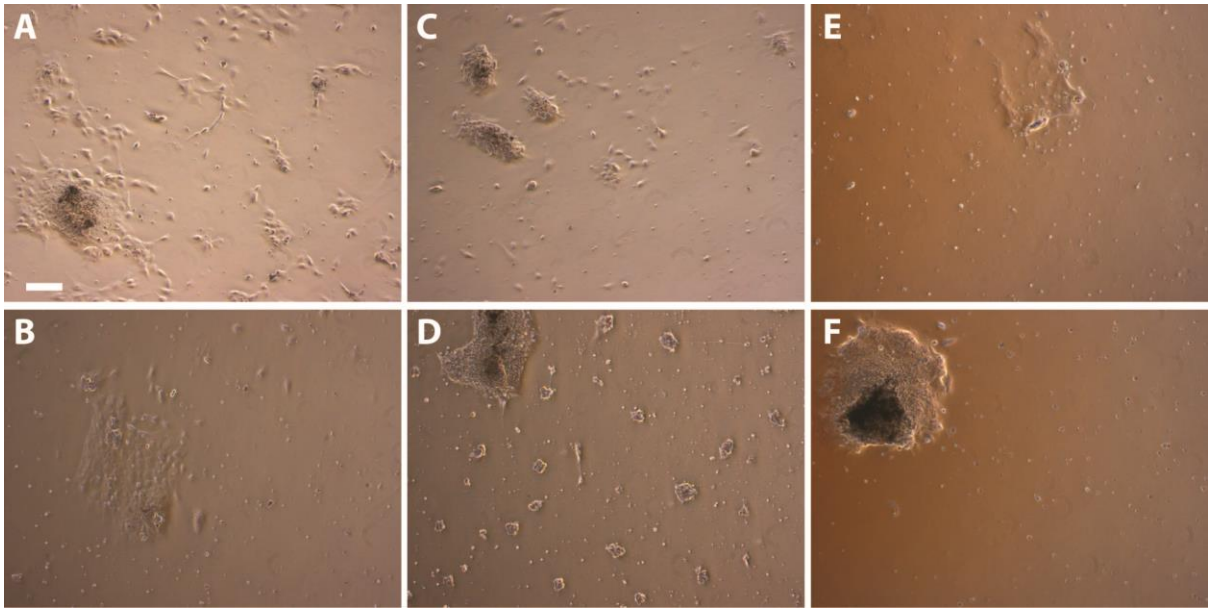

Figure 9 | Bright field images (scale bar = 50µm) showing the lack of neuronal morphology and cell number across all six lines at day 20 post induction. A, B, C, D, E and F show C11WT, C32WT, C79eu, C87eu, C11DS and C18DS, respectively.

For the subsequent attempt, cell lines passaged within days of one another were induced on the same day, however, this yielded similar results when the cells were attempted to be replated back down post day 12 (see figure 10). Again, exact reasons for this failure are unclear.

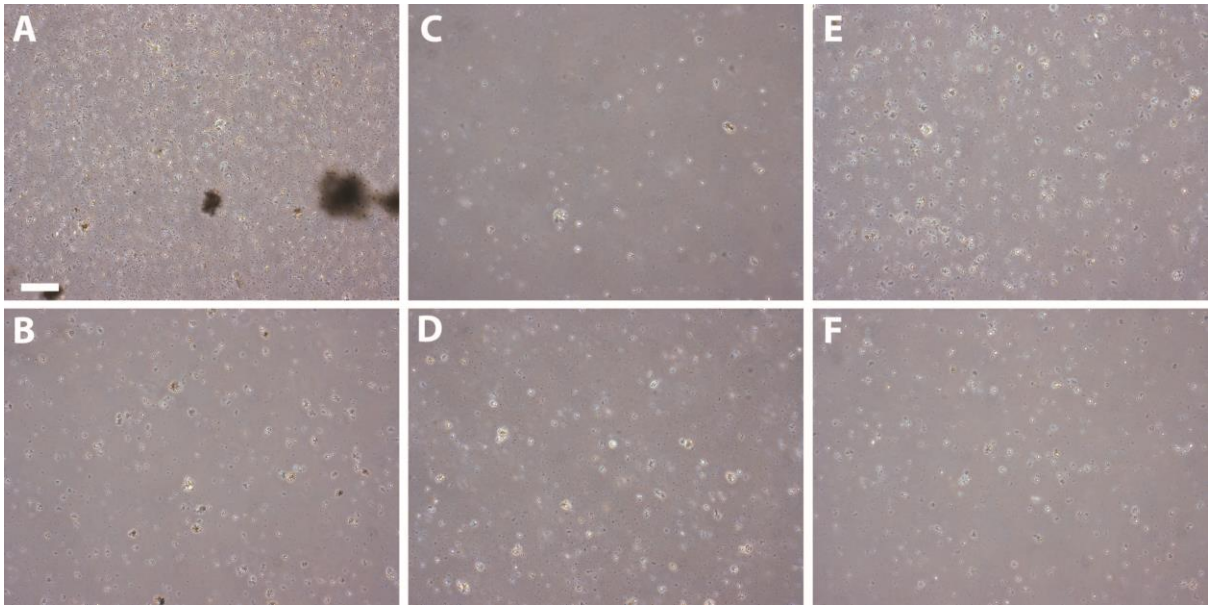

Figure 10 | Bright field images (scale bar = 50µm) of second attempt of coordinated neuronal differentiation, showing mass cell death and lack of any adherent cells at day 14 post induction. A, B, C, D, E and F show C11WT, C32WT, C79eu, C87eu, C11DS and C18DS, respectively.

Immunocytochemistry of MACS of Glial-Like Neuronally-Differentiated C11 Cells

As the proposed alternative to culturing astrocytes in the astrocyte differentiation protocol, magnetic activated cell sorting (MACS) was used in an attempt to sort glia out of mature neuronal cultures. Day 127 cells had been seeded onto coverslips post-MACS at ~30,000 cells/cm^2. And then left to culture for 5 days in order to adequately reattach and form a minimally basic intercellular network. Positive, negative and unsorted immunofluorescence pictures of slides are shown in figure 11. This showed that there appeared to be a significant enough population of A2B5-positive cells in both the positive and negative fractions of the A2B5 MACS sort.

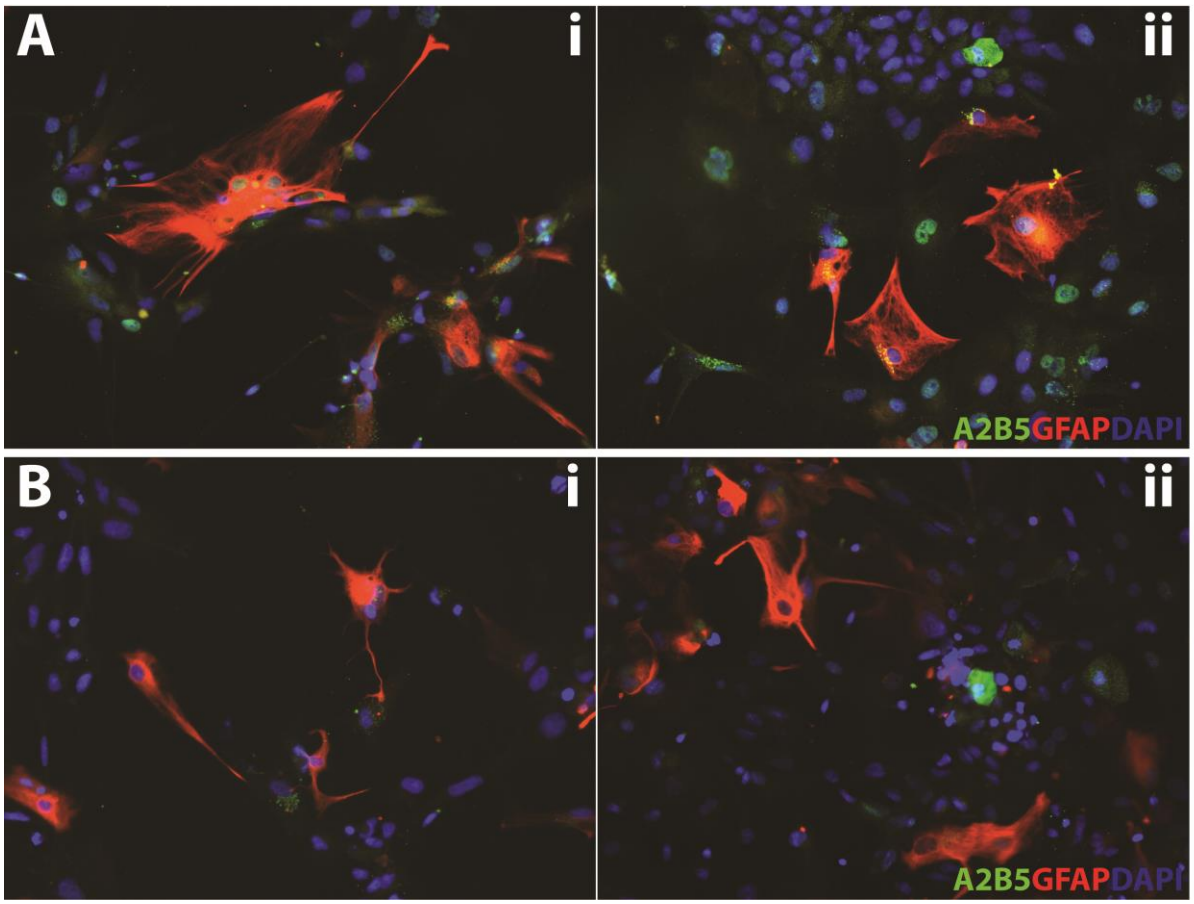

Figure 11 | MACS A2B5-sorted C11 cells from 127 days post neuronal induction. A is the negative fraction, while B shows the positive faction (scale bar = 50µm). Both fractions appear to contain GFAP$^+$ and A2B5$^+$ cells, some double positive, suggesting that the sorting protocol was not successful, but that there are a substantial proportion of GFAP$^+$ and A2B5$^+$ cells in the population of neuronal differentiation that has passed the "glial-switch". For control ICC stains see appendices, figure A1B.

Culture of Neurons in Interaction Device

The interaction device was to be utilised as a platform to measure morphological phenotypes in co-culture. It would allow easy measurement of neuronal processes in the central interaction area with just a simple photograph on a microscope. However, despite repeated attempts at seeding neurons in the interaction device, it was impossible to establish successful

and thriving neuronal populations inside these devices. The cells used were day 100+ post neuronal induction, all from the same cultures that were used to characterise our standard neuronal differentiation protocol (see figures 4 and 5). The main problems were that the device leaked, it was difficult to maintain in sterile conditions and cell attachment was sub-optimal in the device.

On the first and second attempts, before cells were able to be seeded, the device would not secure the media at the interface between glass coverslip and device. For the third attempt, the device was rinsed with 70% ethanol then pre-warmed by placing it (contained in a 10cm petrie dish) in a desiccator (Axyos) at 55°C overnight to increase adherent properties in the PDMS. The wells of the device were then rinsed using 70% ethanol, before being twice rinsed with Neurobasal and then seeded with ECM overnight. As the device was no longer leaking substantially, cells were then seeded into the device and left overnight to settle and adhere. When cells were checked under the microscope the following day there was mass cell death. Given that the device had to be removed from sterile conditions, and the cell culture is antibiotic-free, it was assumed that the cell death may have been due to contamination caused by overnight incubation of the device in the desiccator (despite rinsing the device with 70% ethanol). This process was thus repeated, but without placing the device in the desiccator and instead transferring it an incubator. Despite this change, there was ubiquitous cell death when the cells were seeded this time again (see figure 12).

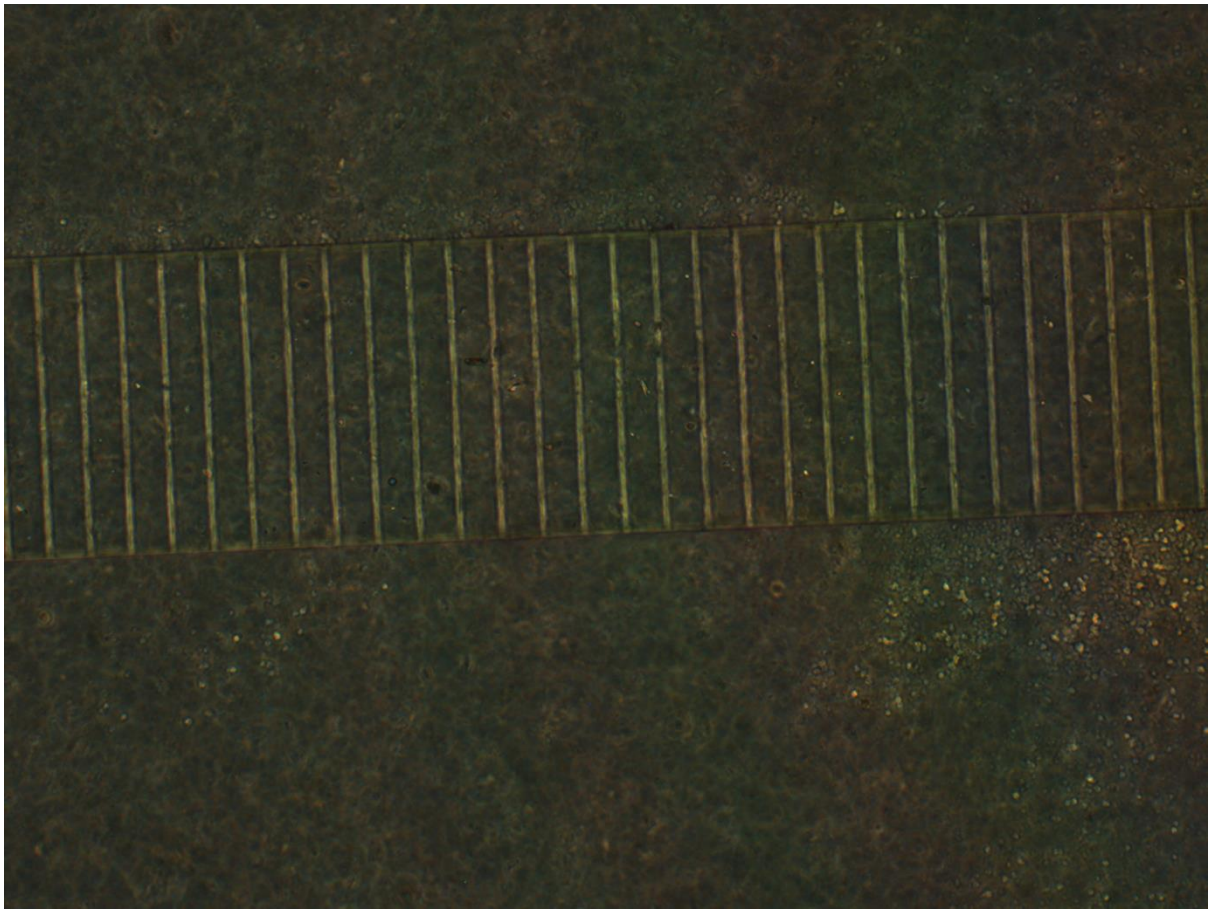

Figure 12 | Bright field image of neurons seeded in interaction device (scale: channels are 3µm across and 100µm long). No survival of neurons was observed. The cells that were present were apoptotic and did not appear to adhere to the ECM-coated glass surface.

For the next attempt, it was suggested that the PDMS material may be harbouring leachable molecules that are toxic to the cells. Therefore, to rid the devices of leachables, the devices were autoclaved before being rinsed with 70% ethanol and seeded with ECM on the glass coverslips on which they were mounted. This eliminated the step of having to warm them overnight since they were heated in the autoclave to increase hydrophilic properties of the device's PDMS material. This time, when neurons were seeded into the cells, there was some survival seen in the wells, however this was not observed in the 10µm-high areas either

side of the channels, in those areas only cell death was observed (see figure 13). By this time, the project was coming to a close and the testing was unable to be continued.

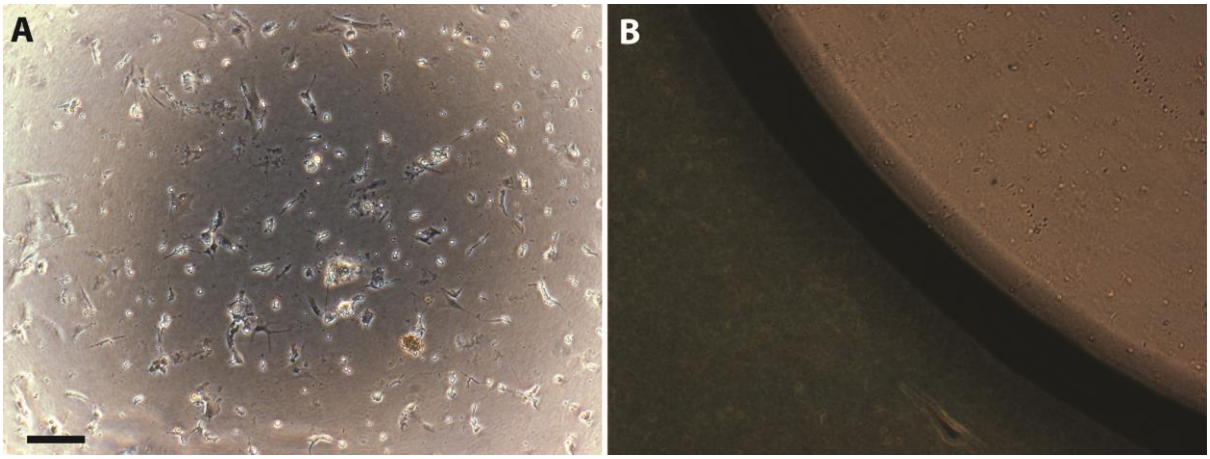

Figure 13 | Bright field photos of in the well of an interaction device (scale bar = 50µm). A shows surviving neuronal differentiation cells inside the well – this was the first time in this project that cells successfully adhered to the ECM-coated coverslips. Although survival is not as optimal as in standard culture, there is clear neuronal morphology across a significant proportion of the cells in the well. B shows the area where the well transitions into the low profile, 10µm-high area of the device that feeds into the 3µm-high interaction channels. There appeared to be only cell death here in the transition area, suggesting the neurons thrive better in an uncovered part of the well with more clearance.

Depolarisation of Mature Neuronal Cultures

Characterisation of Modified Neuronal Differentiation Protocol

The cells used for the depolarisation assay had to be characterised in order to demonstrate depolarisable potential since the protocol was modified from our established neuronal

differentiation protocol. To do this, a similar array of antibodies to those used for the first round of ICC staining (see figures 4 and 5) of our established neuronal differentiation protocol was used on the day 164 neurons of this modified protocol (see figure 14). The immunofluorescence images show that there are extensive βIIItubulin^{+} networks in cultures, as well as s100β^{+} and GFAP^{+} cells in and around the βIIItubulin^{+} network. Photos also demonstrated that there were a small number of A2B5^{+} cells, distinct from the GFAP^{+} populations and that there was elaborate punctate staining for PSD95^{+} synapses. These data confirmed that the neuronal differentiation was proceeding as expected, akin to the standard neuronal differentiation protocol and that cells were ready and mature enough for depolarisation.

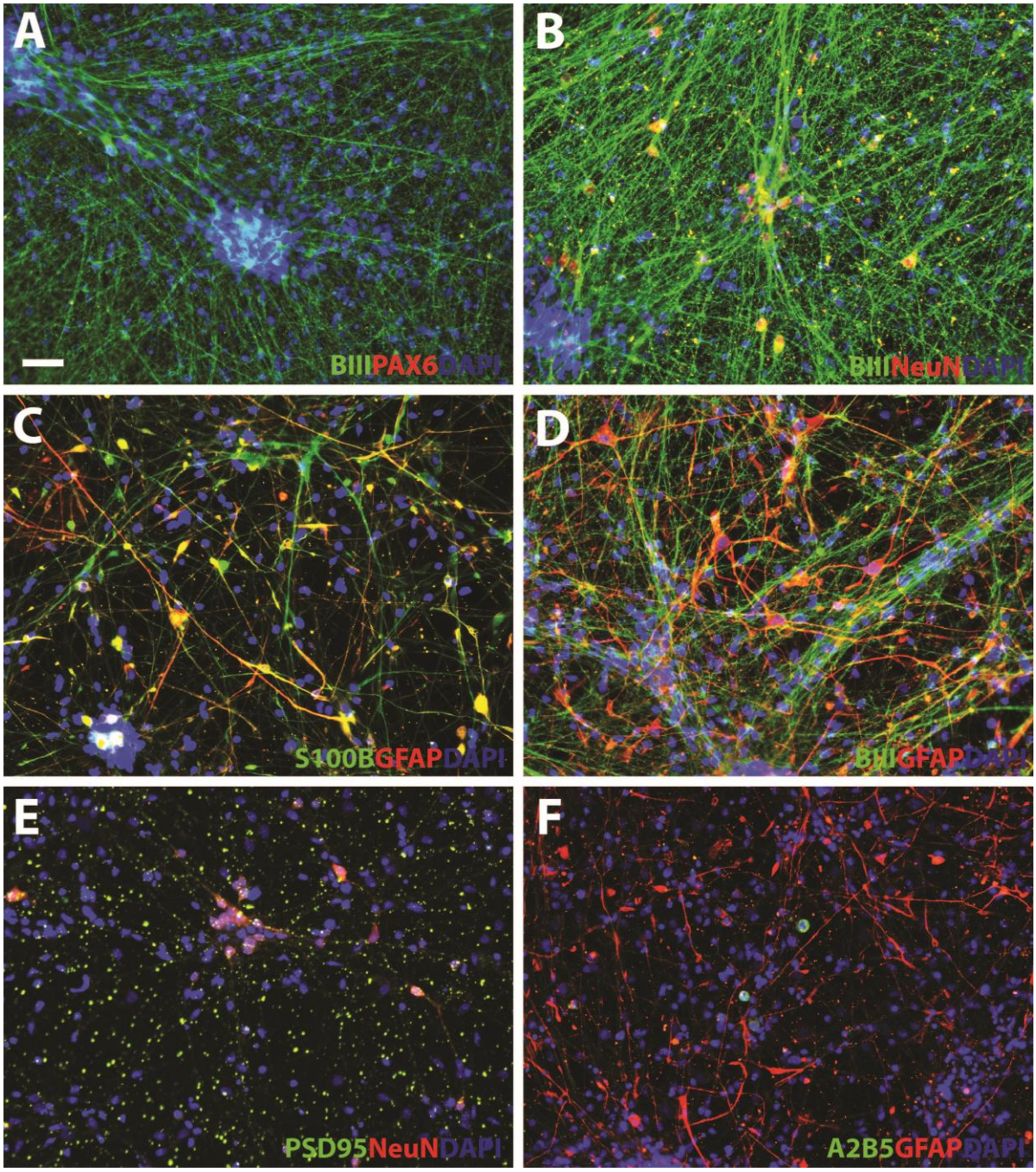

Figure 14 | Immunofluorescence images of ICC of mature neuronal cultures 164 days post induction of neuronal differentiation (scale bar = 50µm). A shows that there is extensive βIIItubulin^{+} neuronal networks with absence of Pax6^{+} progenitors in neurospheres. B shows persistence of some NeuN^{+} positive cells in elaborate βIIItubulin^{+} neuronal networks. C shows that there are s100β^{+}/GFAP^{+} cells as well as s100β^{+}/GFAP^{-} cells in the neuronal cultures, while in D it can be seen that these GFAP^{+}

cells are distributed in and amongst the βIIItubulin$^+$ network. E demonstrates that there is PSD95 synaptic staining both proximal and distal to NeuN$^+$ cells. F shows that there are a small number of A2B5$^+$ cells in culture and that these are distinct from the GFAP$^+$ cells that are present. For control ICC stains see appendices, figure A1.

Upregulation of IEGs to Confirm Depolarisation Activity

A set of immediate early genes (IEGs) was chosen to assess depolarisation induced transcriptional changes following the addition of isotonic glutamate (isoGlut) or KCl (isoKCl) solutions for three hours on day 150 neuronal cultures. Data were analysed in GraphPad Prism using one-way ANOVA on qRT-PCR performed in technical triplicate for each treatment within each gene to compare whether the means of each treatment were statistically significant compared to the isotonic control solution (isoCtrl).

It was found that a number of these key genes were significantly upregulated (see figure 15). The most prominent, cFOS (Sukhatme et al., 1988), showing significant upegulation in both KCl (isoKCl) and glutamate (isoGlut) treatment groups compared to control (isoCtrl) treatment. The other genes showed significant upregulation for either one or none of the two depolarisation treatments (ARC and EGR1 for glutatmate, Neuritin for KCl, and PLAT did not show any significant difference between treatments). These results confirmed that there was depolarisation-induced IEG transcriptional activity triggered with both solutions in at least a portion of the cells in culture.

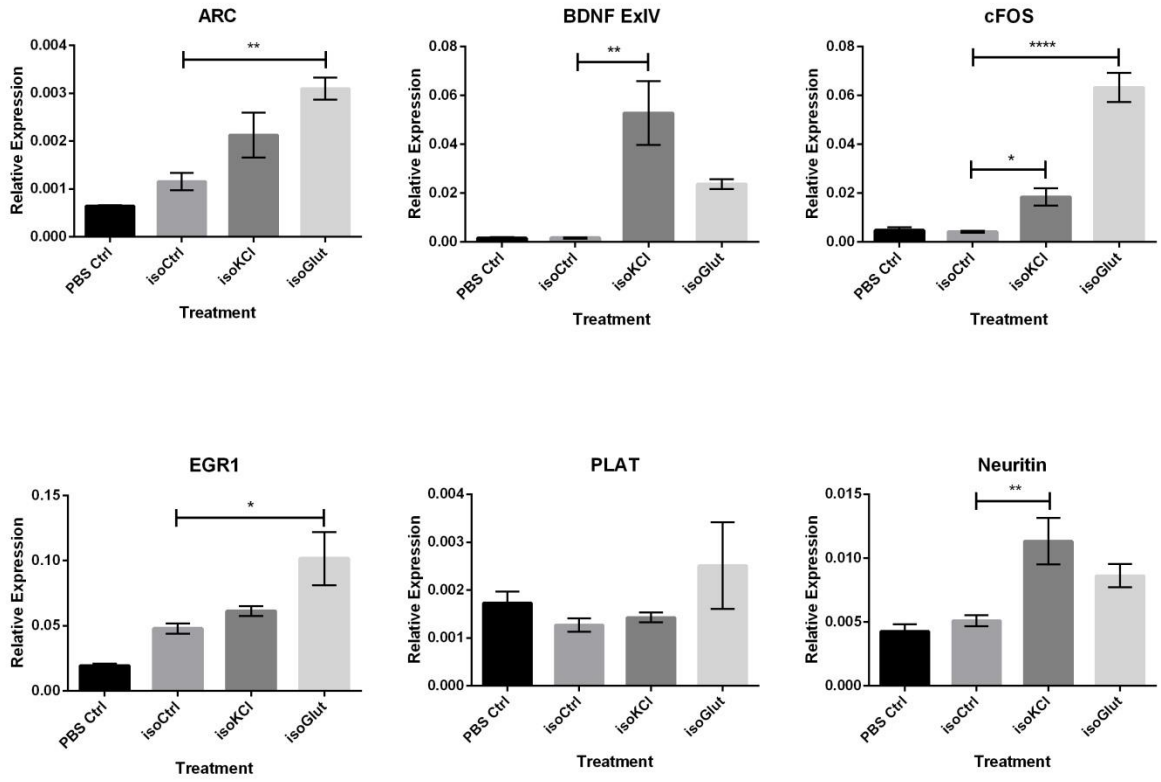

Figure 15 | Graphs of expression analysis performed using qPCR for six immediate early genes (IEGs) (expression relative to GAPDH). These show that for glutamate treatment (isoGlut), ARC ($p = 0.0028$), cFOS ($p < 0.0001$) and EGR1 ($p = 0.0182$) were significantly upregulated compared to the isoCtrl treatment, and for KCl treatment (isoKCl), BDNF ExIV ($p = 0.0015$), cFOS ($p = 0.0491$) and Neuritin ($p = 0.0091$) were significantly upregulated compared to the isoCtrl treatment.

Expression of DNMT3a and DNMT3b in depolarised neuronal cultures

The expression patterns of both DNMT3a and DNMT3b do not appear to follow any definable pattern post depolarisation. Figure 16 shows qPCR results of DNMT3a and DNMT3b at each time point across the four replicates.

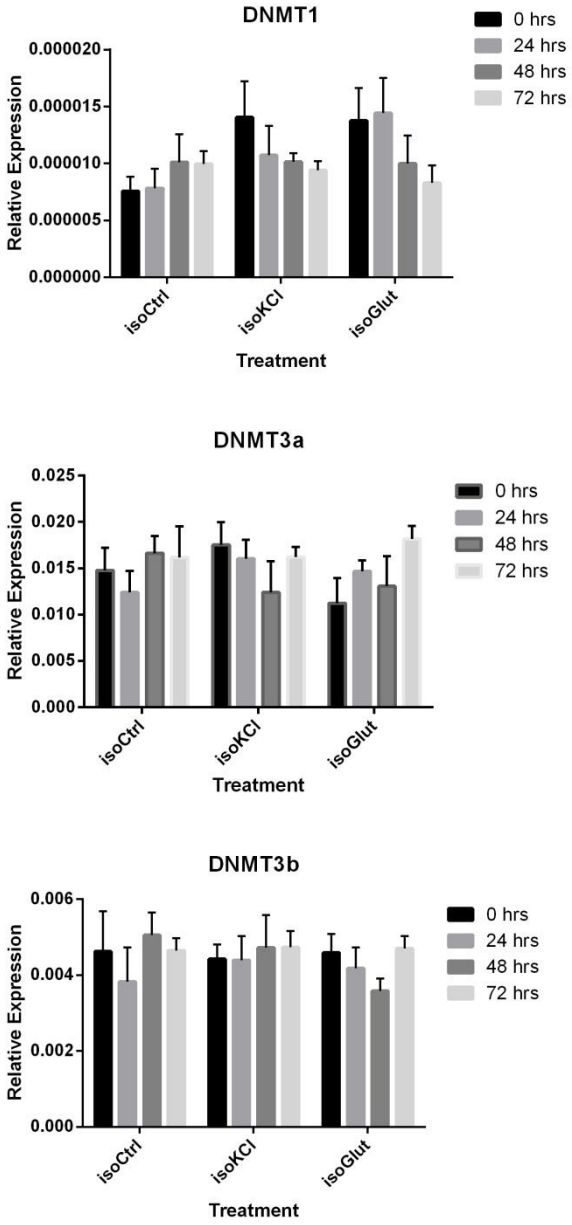

Figure 16 | Graphs of expression analysis performed using qPCR for DNMT genes (expression relative to GAPDH). There does not appear to be any identifiable trend in the graphs, and no relevant statictially significant interactions or correlations could be found.

Since there was no significant alteration to the expression of the DNMT genes 24 and 48 hrs after depolarisation we wished to assess whether the IEGs had appropriately downregulated

after depolarisation. Therefore, qPCR was performed using primers for two of the six IEGs, BDNF ExIV and cFOS at 24 and 48 hrs. The qPCR was performed on all four replicates to identify whether there were individual replicates that were not depolarising. This was done because there was no trend seen in the expression data for the DNMT genes in either pooled statistical analsysis (as seen above in figure 16) or separate analysis of the time course for each replicate (data not shown). It was found that both cFOS and BDNF ExIV expression appeared to show a trend of upregulation for KCl treatment in most replicates, but glutamate treatment only appeared to upregulate cFOS in some replicates (see figure 17). Statistics were unable to be performed on these due to time constraints as only one yield of cDNA per sample was used. Despite this, these data still show clear, identifiable trends.

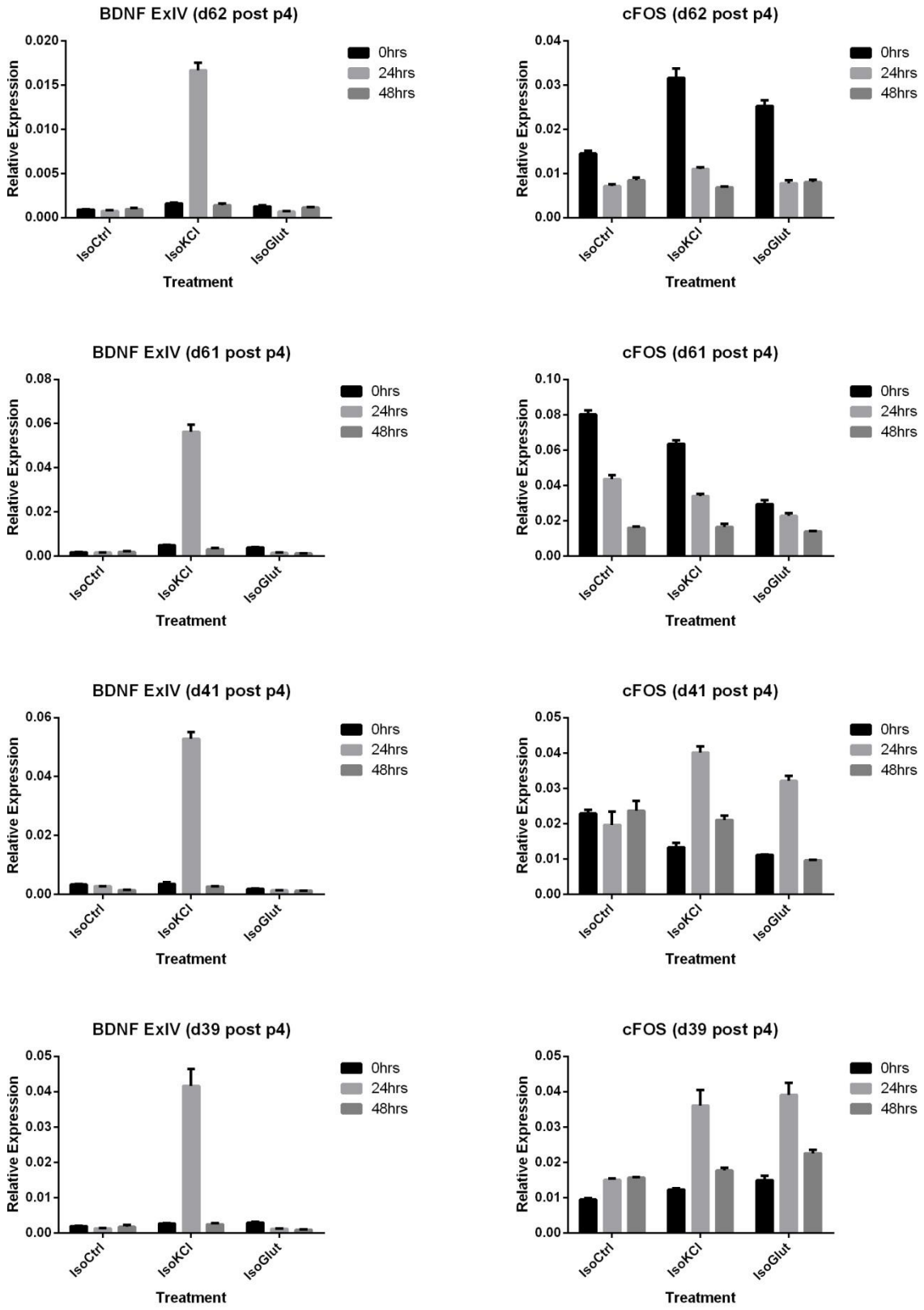

Figure 17 | Graphs of expression analysis performed using qPCR for two IEGs (expression relative to GAPDH). These show that cells appeard to be depolarising as

predicted. For glutamate treatment there appears to be a trend of upregulation in the replicates of 39 and 41 days post p4. These show a trend of upregulation at 24hrs and then return to near-normal levels at 48hrs, after 24hrs back in regular media. For KCl treatment, both genes appear to show upregulation at 24hrs and then return to near-normal levels at 48hrs in all replicates except for cFOS expression in days 62 and 61 post p4.

Discussion

This project initially set out to achieve two main aims. The first aim was to co-culture control and DS neurons and astrocytes in order to interrogate AD phenotypes in the dish. This was to be achieved by first developing a novel astrocyte differentiation protocol that would produce astrocytes earlier and more efficiently than any existing astrocyte differentiation protocols. These astrocytes would then be used with neurons from our existing neuronal differentiation protocol to co-culture the control and DS neurons and astrocytes.

The second aim was to depolarise mature neuronal differentiation cultures and assess the expression of IEGs and DNMT genes in order to determine the underlying mechanisms involved in transmitting and recording neuronal activity into epigenetic changes in the nucleus of the neuron. This was to be achieved by using a novel, modified method of neuronal differentiation to produce mature, depolarisable neurons, and then depolarising these cells with KCl and glutatmate to assess how these two agents can affect epigenetic change in the neuronal genome.

The first aim was largely problematic. The astrocyte differentiation protocol proved to be unable to produces astrocytes, despite repeated attempts with modified approaches each time (see figures 6, 7 and 8). The alternate plan to use A2B5 MACS to sort astrocytes out of late neuronal cultures cells for co-culture astrocytes and neurons was not shown to be efficient or specific enough and by then it was too late in the project to continue to try this (see figure 11). Success was however found in the characterisation of late neuronal differentiation cultures by ICC staining. Cells were shown to form large numbers of synaptic connections, with both glia and neurons present in culture (see figures 4 and 5).

The second aim was more successful in achieving what was set out. Late neuronal cultures were able to be characterised using ICC and qPCR, and a novel, modified method of neuronal differentiation was characterised and depolarised to assess expression of DNMT

genes across four time points over 72 hours with the two different depolarisation agents, KCl and glutamate. Transient DNMT upregulation as was previously observed in mouse primary neurons were not observed in our experiments despite the fact that we confirmed robust upregulation of mRNA expression of two IEGs, indicating that the neurons did in fact appear to be depolarising. Each set of results will now be discussed below in full to expand on the outcomes and consequences of what was outlined above.

Cell Cycle Analysis of All hiPSC Lines

During hiPSC culture, one reason concurrent differentiation of all six lines proved difficult was the disparate growth rate of DS lines (C11DS and C18DS) which appeared slower than that of the control lines (C79eu, C87eu, C11WT, C32WT). In an attempt to identify the reason behind this, a cell cycle EdU incorporation assay was used. The cell cycle analysis of the six hiPSC lines demonstrated that they were similar in their apparent rate of proliferation (see figure 1). It did appear however that there may be a trend showing that there are more cells in G_1/G_0 for the euploid lines than in the other four, however, as the cell cycle assay was not performed in replicate, it was impossible to statistically compare the proliferation rate of each cell line and establish whether there was a significant difference between DS and control lines as initially postulated. In future experiments it would be appropriate to also assess cell death/apoptosis (i.e. via Terminal deoxynucleotidyl transferase dUTP nick end labelling (TUNEL) using FACS) in order to determine whether the different growth rates observed are due to increased cell death rates. It was already shown to be the case that there is increased levels of apoptosis in our DS neuronal differentiation cultures compared to control (Briggs et al., 2013b), however this has not been characterised while cells are still in the undifferentiated hiPSC state.

Astrocyte Differentiation

The astrocyte differentiation protocol was developed based on a protocol published by the Zeng lab in 2013 (Shaltouki et al., 2013), as well as with experience gained from our own neuronal differentiation protocols. Given that most astrocytes differentiation protocols start with neural progenitor generation via utilisation of the early stages of existing neuronal differentiation protocols (Shaltouki et al., 2013, Williams et al., 2014, Juopperi et al., 2012) we took a similar approach. Unfortunately, the protocol repeatedly failed and, no astrocytes were able to be produced with this protocol. Instead we attempted to use astrocytes generated from late neuronal differentiation cultures using the A2B5 MACS protocol. However, this was also unsuccessful, perhaps because the antibody beads were too old, or the column filters was not suitable for astrocytes morphology – the exact reason is not clear.

To ensure better success I would propose a small number of changes that may lead to more successful efficient generation of astrocytes. First of all, a supplement such as N2 or B27 (both from Life Technologies) should be used in the astrocyte differentiation media containing Neurobasal, LIF, EGF and GlutaMax, from the time at which the astrocyte differentiation protocol diverges from our neuronal differentiation protocol (day 6). Given that both N2 and B27 have been shown to be used in astrocyte differentiation protocols, the supplement could be either N2 (Williams et al., 2014), or B27 (Shaltouki et al., 2013), or possibly both. Given that our proposed protocol was based upon that of Shaltouki et al. however (Shaltouki et al., 2013), it would be most logical to use B27, as they have exemplified. This was probably the first reason that our modified astrocyte differentiation protocol was not successful.

The other vital change that should be made is a later transition to astrocyte precursor-generating medium. It would be more logical, given the findings and protocols of other research groups to generate astrocytes from day 12 or 18 post induction (Emdad et al., 2012,

Shaltouki et al., 2013, Williams et al., 2014), rather than as early as day 6 post induction as proposed by our protocol. The onset of glial expansion (first astrocytes, then oligodendrocytes) has been shown to be later than neurons, after the initial stage of the peak of expansion of the neuronal population, which is much later *in vivo* than what is happening at day 6 *in vitro* as far as is known (Rowitch and Kriegstein, 2010), especially from what has been shown in protocols similar to our neuronal differentiation protocol (Kim et al., 2010, Chambers et al., 2009, Briggs et al., 2013b).

Indeed, it is possible that the relevant cytokine receptors necessary for differentiation into astrocytes (that we are attempting to target with LIF and EGF) are in fact not present or active at these early stages of development. This could mean that our initial aim of attempting to make an astrocyte differentiation protocol that produces astrocytes faster and more efficiently than existing protocols is in fact impossible if the right receptors are not there until later. For a better understanding of the intracellular mechanics of astrocyte differentiation, this would have to continue to be tested with the aforementioned alterations to the protocol.

A2B5 MACS: An Alternate Method to Generating Astrocytes for Co-culture

In the case that the direct astrocyte differentiation protocol would not produce, or would not efficiently produce astrocytes, our alternate plan was to take late neuronal cultures which had passed the "glial-switch" (Rowitch and Kriegstein, 2010) stage of development and MACS-sort them for the astrocyte marker A2B5 and then co-culture these sorted cells with late NCAM MACS-sorted cells, also from our neuronal differentiation protocol. This would at least give a defined start population of co-cultured astrocytes and neurons. However, the MACS protocol for A2B5-sorting produced dubious results, insofar as not appearing to be able to sort $A2B5^{+}$ cells from $A2B5^{-}$ cells, it was then too late to continue trialling methods of astrocytes isolation, either by differentiation of MACS.

In the A2B5 MACS protocol, it was expected that cells would be some proportion of $GFAP^+$ cells in both fractions, but only the $A2B5^+$ fraction would harbour $A2B5^+$ cells; however, surprisingly, both fractions appeared to have almost the same proportion of $GFAP^+$ and $A2B5^+$ cells. Unfortunately, given the time restraint on the project, this technique was unable to be repeated preventing us from determining whether the antibody beads were unreliable or whether this was caused by inappropriate harvesting and destruction of the A2B5 antigen on the astrocytes.

Difficulties in co-ordinating concurrent differentiation of all six hiPSC lines

As has already been touched on, one reason concurrent differentiation of the six cell lines was so difficult is that they do not all expand at the same rate. Unfortunately, even when this problem of expansion was finally overcome for a brief period, there were a number of instances where cells would unexpectedly die or simply not plate down, as shown in figures 9 and 10. The exact reason for this mass cells death is unknown, but there are a number of potential explanations. Firstly, the cells may not have been aggregated enough during the time in ultra-low cluster plates for formation of neurospheres. This would mean that the cell clump size was too small to aggregate with other clumps and form neurospheres – a consequence sometimes observed if not enough care is taken to ensure minimal separation of cell colony clumps during passaging. In addition to this, the acquisition of neuronal differentiation as a consistently reproducible protocol and technique was initially a very difficult obstacle to overcome at the beginning of the project. This was not unknown coming into the project, but it played a large role in the delay of initial and later success with the neuronal differentiation protocol.

Interestingly, towards later stages of the protocol, from around 70 days post induction onwards, neuronal differentiation cultures would sometimes appear to become overgrown by

glial-like cells. The exact reason for this, however, was not defined. This could have been able to be attributed to cell density; however cell density was not recorded for the majority of the project – a significant oversight in hindsight given that it is known that density is important in differentiation (Chambers et al., 2009). Through simple microscopic observation, it did appear that the cell density was lower in those cultures whose morphology would transition from neuronal to gliogenic at later stages in the protocol. This is an important indication that cell density is an important factor in neuronal differentiation (as mentioned above), as has been reported in previously published protocols (Chambers et al., 2009, Kim et al., 2010).

Characterisation of Late Neuronal Differentiation in hiPSC lines

Before the final time point of ICC taken from the neuronal differentiation, a number of different ICC assays were processed along the way. There would have been robust characterization all along the differentiation pathway were it not for a number of these failed ICC assays. This was simply due to a lack of technical expertise from the outset, which was overcome with experience towards the end of the project.

Although there was substantial failure in initiating concurrent neuronal differentiation across all six hiPSC lines (C11WT, C32WT, C79eu, C87eu, C11DS and C18DS) (see figures 9 and 10), neuronal differentiation was able to be completed and characterised in the wild-type cell lines, C11WT and C32WT. This was able to be achieved at later time points along the differentiation timeline after sufficient experience in ICC and neuronal differentiation was acquired (see figures 3, 4 and 5). The results from ICC show that there is robust synaptogenesis and synaptic maturation occurring, indicated by the presence of synapsin-1 (Ferreira et al., 1998, Perlini et al., 2011) and PSD95 (El-Husseini et al., 2000), including mature inhibitory interneurons indicated by the presence of Gephyrin^{+} cells (Levi et al., 1999,

Tretter et al., 2008), supported by SV2 staining indicating presence of inhibitory synapses across a large section of the cell population (Nowack et al., 2010). The vast majority of cells appear to be of neuronal identity, indicated by the presence of βIIItubulin, but there was also a number of glia present, indicated by the expression of GFAP and S100β in culture, and low levels of A2B5 expression in some cells.

Neuronal Culture in the Interaction Device

The interaction device had been shown to be a useful tool for interrogation of neuronal growth and development (Taylor et al., 2005). Neurons were able to eventually be cultured in the wells of the device; however these neurons did not survive in the most important part of the device where the axonal growth was to be measured (see figures 12 and 13). This may have been caused by persistence of leachable toxins harboured in the PDMS material of which the device was made, but may also be due to the neurons not having enough space for growth with only 10μm of clearance. For future attempts of culture of neurons in this device, it would be important to maintain a sterile environment inside the device to avoid contamination of cells. The addition of small concentrations of antibiotics (such as PenStrep) may aid in ensuring the device remains infection-free. The differentiation protocol is technically antibiotic-free; however, the use of antibiotics in neuronal culture is widely accepted as standard practice. The exact reasons for failure are still unclear, but successful culture of neurons in this device has already been demonstrated, so it is not an unrealistic expectation to culture neurons in this device (Taylor et al., 2005).

A modified protocol of neuronal differentiation for enhanced facilitation of neuronal patterning in development

The next stage of the project then transitioned to depolarising neurons matured in culture. The objective of this next stage was to determine whether depolarised neurons underwent changes in methylation mechanics that may be involved in the transmission and recording of neuronal activity in the epigenetic landscape. The neuronal differentiation protocol was modified by extending the time that the cells were cultured as neurospheres (up to day 60, instead of up to day 12 of the protocol) (Kim et al., 2010, Briggs et al., 2013b) as an attempt to enrich cultures for a greater number of diverse, depolarisable neuronal subtypes, potentially formed during internal patterning in the neuronspheres as has been shown with neuronal EB culture in the past (Lancaster et al., 2013). ICC stains of the cells showed that there was synaptogenesis occurring with expression of PSD95, and that the make up of glia and neurons in culture appeared similar to the standard differentiation protocol used in this investigation (see figures 4, 5 and 14). The true test of depolarisability came with use of qPCR to identify upregulation of immediate early gene (IEG) mRNA expression post depolarisation, which showed that at least a portion of the cells in culture did appear to be depolarising (see figure 15).

Verification of Depolarisation Activity: Upregulation of IEGs

The cells produced from this alternate protocol had to be shown to be depolarisable in order for the depolarisation experiment to be worthwhile. It has been shown that not balancing the overall salt concentration can have effects on the production of particular intracellular proteins (Kilbourne et al., 1991). For this reason the depolarisaiton solutions used in this project were adjusted so that their overall osmolarity matched (see table 1). This ensured that

the KCl depolarisation solution was isotonic, and that the effects of the glutamate and control solutions were able to be compared to those of KCl.

For 150 day old neurons that had been exposed to the depolarisation solution for 3 hours, qPCR analysis was performed to assess the expression of six IEGs in order to ascertain whether depolarisation was occurring. The results showed a trend of upregulation for one or more of the two treatments (isoKCl and isoGlut) in five of the six genes (see figure 15), suggesting that at least a portion of the cells in culture were depolarising. The cells were therefore ready for the depolarisation assay.

Analysis of cells and gene expression post-depolarisation

First, it had to be confirmed that there were cells depolarising in culture, as we had seen in the initial IEG test on the late neuronal differentiation cultures (see figure 14). We ran qPCR on two of these genes, cFOS and BDNF ExIV, as these had been discussed in reference to confirmation of cell depolarisation in the literature (Sharma et al., 2008, Sukhatme et al., 1988) and the number of samples was too great to be able to adequately analyse expression of all six IEGs. The two IEGs used showed that there was a trend of upregulation post depolarisaiton for both genes across the mojoriy of the replicates for KCl, but only across two replicates in cFOS for glutatmate treatment (see figure 17). This still appeared to confirm that the majority of neuronal differentiation cultures contained at the least a portion of identifiably depolarisable cells. These differences in IEG upregulation between KCl and Glutamate may be due to the fact that each is exciting different depolarisable neuronal sub-types (Takamori et al., 2000, Sauer et al., 2012).

The expression of the genes DNMT1, DNMT3a and DNMT3b after treatment with KCl and glutatmate was then analysed using qPCR. The data appeared not to show any significant alteration of mRNA expression of these genes compared to the isoCtrl treatment at

any of the time points (see figure 16). It was not clear why exactly this was given that there had been reports of depolarisation and neuronal activity affecting DNMT gene expression (Sharma et al., 2008, Feng et al., 2005, Guo et al., 2011). We would postulate, however, that because there are a number of different cell types in these cultures (see figure 14), it is possible that the mRNA signal of DNMT gene regulation of depolarising neurons is drowned out by the RNA signal of all of the other neurons and glia in culture. It has also been shown that DNMT3a and 3b activity is higher in dividing neurons (Feng et al., 2005, Feng et al., 2010), indicating that this signal may also be contributing to masking the mRNA signal of the possible downregulation of DNMT expression in post-mitotic, depolarising neurons (Sharma et al., 2008).

For further investigation, an important step would be to use a positive control of a population of cells with a known proportion of depolarisable cells, such as those used in previous studies (Sharma et al., 2008). However, it may be possible that the mechanisms driving epigenetic imprinting of memory and learning could be different between mouse and human, either occurring through a different mechanism or pathway, or by different kinetics – a plausible explanation that may go some way to explaining the significant difference in cognitive ability between humans and other animals, given that human cognition is believed to be intrinsically linked to epigenetic imprinting (Day and Sweatt, 2011). In this case, a culture of mouse control neurons would not be able to teach us any more about human epigenetic memory imprinting. Instead, it could simply be due to neuronal maturity in our cultures. We know that cells need to mature to be able to depolarise (Spitzer, 2006), so it is entirely possible that the cells we generated in culture were too young to be able to observe activity-induced DNMT activity.

Conclusions

Although the aims of the project were not fully achieved, significant advances – including the characterisation of mature neuronal differentiation, and the differentiation and culture of mature, depolarisable neurons – were achieved. These enabled the interrogation of the mRNA expression of DNMT genes post depolarisation. This was done to determine whether these genes played a role in the transmission and recording of neuronal activity through epigenetic changes. The results remain inconclusive, but there is now a clear window in which we know to look, indicated by the transient upregulation of IEG expression. In addition to this, the unsuccessful attempts at astrocyte differentiation and co-ordinated DS and control neuronal differentiation leave much information on how to avoid these failings in future. These lessons will be valuable to all those who follow this path of investigation in the future.

Finally, it must be mentioned that in our collaboration with Professor Lister, the samples from the depolarisation experiment are currently being assessed for activity-induced epigenetic changes. This is not just in changes in DNA methylation however, but also in DNA hydroxymethylation and non-CG DNA methylation changes as well. It must be noted that hiPSC-derived neurons are the only way that basic features of cognition and neurological disease can be systematically investigated with an *in vitro* human neuronal model, so the potential for this approach to uncover significant steps forward in our understanding of memory and cognition is substantial.

References

ALDINGER, K. A., PLUMMER, J. T. & LEVITT, P. 2013. Comparative DNA methylation among females with neurodevelopmental disorders and seizures identifies TAC1 as a MeCP2 target gene. *J Neurodev Disord,* 5**,** 15.

BELHAGE, B., HANSEN, G. H. & SCHOUSBOE, A. 1993. Depolarization by K+ and glutamate activates different neurotransmitter release mechanisms in GABAergic neurons: vesicular versus non-vesicular release of GABA. *Neuroscience,* 54**,** 1019-34.

BRIGGS, J. A., MASON, E. A., OVCHINNIKOV, D. A., WELLS, C. A. & WOLVETANG, E. J. 2013a. Concise review: new paradigms for Down syndrome research using induced pluripotent stem cells: tackling complex human genetic disease. *Stem Cells Transl Med,* 2**,** 175-84.

BRIGGS, J. A., SUN, J., SHEPHERD, J., OVCHINNIKOV, D. A., CHUNG, T. L., NAYLER, S. P., KAO, L. P., MORROW, C. A., THAKAR, N. Y., SOO, S. Y., PEURA, T., GRIMMOND, S. & WOLVETANG, E. J. 2013b. Integration-free induced pluripotent stem cells model genetic and neural developmental features of down syndrome etiology. *Stem Cells,* 31**,** 467-78.

CHAMBERS, S. M., FASANO, C. A., PAPAPETROU, E. P., TOMISHIMA, M., SADELAIN, M. & STUDER, L. 2009. Highly efficient neural conversion of human ES and iPS cells by dual inhibition of SMAD signaling. *Nat Biotechnol,* 27**,** 275-80.

DAY, J. J. & SWEATT, J. D. 2011. Epigenetic mechanisms in cognition. *Neuron,* 70**,** 813-29.

ECONOMICS, D. A. 2011. Dementia Across Australia: 2011-2050. Alzheimer's Australia.

EL-HUSSEINI, A. E., SCHNELL, E., CHETKOVICH, D. M., NICOLL, R. A. & BREDT, D. S. 2000. PSD-95 involvement in maturation of excitatory synapses. *Science,* 290**,** 1364-8.

EMDAD, L., D'SOUZA, S. L., KOTHARI, H. P., QADEER, Z. A. & GERMANO, I. M. 2012. Efficient differentiation of human embryonic and induced pluripotent stem cells into functional astrocytes. *Stem Cells Dev,* 21**,** 404-10.

FENG, J., CHANG, H., LI, E. & FAN, G. 2005. Dynamic expression of de novo DNA methyltransferases Dnmt3a and Dnmt3b in the central nervous system. *J Neurosci Res,* 79**,** 734-46.

FENG, J., ZHOU, Y., CAMPBELL, S. L., LE, T., LI, E., SWEATT, J. D., SILVA, A. J. & FAN, G. 2010. Dnmt1 and Dnmt3a maintain DNA methylation and regulate synaptic function in adult forebrain neurons. *Nat Neurosci,* 13**,** 423-30.

FERREIRA, A., CHIN, L. S., LI, L., LANIER, L. M., KOSIK, K. S. & GREENGARD, P. 1998. Distinct roles of synapsin I and synapsin II during neuronal development. *Mol Med,* 4**,** 22-8.

GUO, J. U., MA, D. K., MO, H., BALL, M. P., JANG, M. H., BONAGUIDI, M. A., BALAZER, J. A., EAVES, H. L., XIE, B., FORD, E., ZHANG, K., MING, G. L., GAO, Y.

& SONG, H. 2011. Neuronal activity modifies the DNA methylation landscape in the adult brain. *Nat Neurosci,* 14**,** 1345-51.

HU, J., AKAMA, K. T., KRAFFT, G. A., CHROMY, B. A. & VAN ELDIK, L. J. 1998. Amyloid-beta peptide activates cultured astrocytes: morphological alterations, cytokine induction and nitric oxide release. *Brain Res,* 785**,** 195-206.

ITAGAKI, S., MCGEER, P. L., AKIYAMA, H., ZHU, S. & SELKOE, D. 1989. Relationship of microglia and astrocytes to amyloid deposits of Alzheimer disease. *J Neuroimmunol,* 24**,** 173-82.

JUOPPERI, T. A., KIM, W. R., CHIANG, C. H., YU, H., MARGOLIS, R. L., ROSS, C. A., MING, G. L. & SONG, H. 2012. Astrocytes generated from patient induced pluripotent stem cells recapitulate features of Huntington's disease patient cells. *Mol Brain,* 5**,** 17.

KILBOURNE, E. J., MCMAHON, A. & SABBAN, E. L. 1991. Membrane depolarization by isotonic or hypertonic KCl: differential effects on mRNA levels of tyrosine hydroxylase and dopamine beta-hydroxylase mRNA in PC12 cells. *J Neurosci Methods,* 40**,** 193-202.

KIM, D. S., LEE, J. S., LEEM, J. W., HUH, Y. J., KIM, J. Y., KIM, H. S., PARK, I. H., DALEY, G. Q., HWANG, D. Y. & KIM, D. W. 2010. Robust enhancement of neural differentiation from human ES and iPS cells regardless of their innate difference in differentiation propensity. *Stem Cell Rev,* 6**,** 270-81.

LANCASTER, M. A., RENNER, M., MARTIN, C. A., WENZEL, D., BICKNELL, L. S., HURLES, M. E., HOMFRAY, T., PENNINGER, J. M., JACKSON, A. P. & KNOBLICH, J. A. 2013. Cerebral organoids model human brain development and microcephaly. *Nature*.

LEVI, S., CHESNOY-MARCHAIS, D., SIEGHART, W. & TRILLER, A. 1999. Synaptic control of glycine and GABA(A) receptors and gephyrin expression in cultured motoneurons. *J Neurosci,* 19**,** 7434-49.

MCCORMICK, D. A., WANG, Z. & HUGUENARD, J. 1993. Neurotransmitter control of neocortical neuronal activity and excitability. *Cereb Cortex,* 3**,** 387-98.

MILLER, C. A. & SWEATT, J. D. 2007. Covalent modification of DNA regulates memory formation. *Neuron,* 53**,** 857-69.

MRAK, R. E. & GRIFFINBC, W. S. 2001. The role of activated astrocytes and of the neurotrophic cytokine S100B in the pathogenesis of Alzheimer's disease. *Neurobiol Aging,* 22**,** 915-22.

NOWACK, A., YAO, J., CUSTER, K. L. & BAJJALIEH, S. M. 2010. SV2 regulates neurotransmitter release via multiple mechanisms. *Am J Physiol Cell Physiol,* 299**,** C960-7.

PARK, I. H., ARORA, N., HUO, H., MAHERALI, N., AHFELDT, T., SHIMAMURA, A., LENSCH, M. W., COWAN, C., HOCHEDLINGER, K. & DALEY, G. Q. 2008. Disease-specific induced pluripotent stem cells. *Cell,* 134**,** 877-86.

PERLINI, L. E., BOTTI, F., FORNASIERO, E. F., GIANNANDREA, M., BONANOMI, D., AMENDOLA, M., NALDINI, L., BENFENATI, F. & VALTORTA, F. 2011. Effects of

phosphorylation and neuronal activity on the control of synapse formation by synapsin I. *J Cell Sci,* 124**,** 3643-53.

ROWITCH, D. H. & KRIEGSTEIN, A. R. 2010. Developmental genetics of vertebrate glial-cell specification. *Nature,* 468**,** 214-22.

SAUER, J. F., STRUBER, M. & BARTOS, M. 2012. Interneurons provide circuit-specific depolarization and hyperpolarization. *J Neurosci,* 32**,** 4224-9.

SHALTOUKI, A., PENG, J., LIU, Q., RAO, M. S. & ZENG, X. 2013. Efficient generation of astrocytes from human pluripotent stem cells in defined conditions. *Stem Cells,* 31**,** 941-52.

SHARMA, R. P., TUN, N. & GRAYSON, D. R. 2008. Depolarization induces downregulation of DNMT1 and DNMT3a in primary cortical cultures. *Epigenetics,* 3**,** 74-80.

SHENG, M. & GREENBERG, M. E. 1990. The regulation and function of c-fos and other immediate early genes in the nervous system. *Neuron,* 4**,** 477-85.

SHI, Y., KIRWAN, P., SMITH, J., MACLEAN, G., ORKIN, S. H. & LIVESEY, F. J. 2012. A human stem cell model of early Alzheimer's disease pathology in Down syndrome. *Sci Transl Med,* 4**,** 124ra29.

SPITZER, N. C. 2006. Electrical activity in early neuronal development. *Nature,* 444**,** 707-12.

STATISTICS, A. B. O. 2012. Causes of Death, Australia, 2010. *In:* STATISTICS, A. B. O. (ed.). Canberra: Australian Bureau of Statistics.

STRUBING, C., AHNERT-HILGER, G., SHAN, J., WIEDENMANN, B., HESCHELER, J. & WOBUS, A. M. 1995. Differentiation of pluripotent embryonic stem cells into the neuronal lineage in vitro gives rise to mature inhibitory and excitatory neurons. *Mech Dev,* 53**,** 275-87.

SUKHATME, V. P., CAO, X. M., CHANG, L. C., TSAI-MORRIS, C. H., STAMENKOVICH, D., FERREIRA, P. C., COHEN, D. R., EDWARDS, S. A., SHOWS, T. B., CURRAN, T. & ET AL. 1988. A zinc finger-encoding gene coregulated with c-fos during growth and differentiation, and after cellular depolarization. *Cell,* 53**,** 37-43.

TAKAMORI, S., RHEE, J. S., ROSENMUND, C. & JAHN, R. 2000. Identification of a vesicular glutamate transporter that defines a glutamatergic phenotype in neurons. *Nature,* 407**,** 189-94.

TAYLOR, A. M., BLURTON-JONES, M., RHEE, S. W., CRIBBS, D. H., COTMAN, C. W. & JEON, N. L. 2005. A microfluidic culture platform for CNS axonal injury, regeneration and transport. *Nat Methods,* 2**,** 599-605.

THIES, W., BLEILER, L. & ALZHEIMER'S, A. 2013. 2013 Alzheimer's disease facts and figures. *Alzheimers Dement,* 9**,** 208-45.

TISCORNIA, G., VIVAS, E. L. & IZPISUA BELMONTE, J. C. 2011. Diseases in a dish: modeling human genetic disorders using induced pluripotent cells. *Nat Med,* 17**,** 1570-6.

TRETTER, V., JACOB, T. C., MUKHERJEE, J., FRITSCHY, J. M., PANGALOS, M. N. & MOSS, S. J. 2008. The clustering of GABA(A) receptor subtypes at inhibitory synapses is facilitated via the direct binding of receptor alpha 2 subunits to gephyrin. *J Neurosci,* 28**,** 1356-65.

WANG, T., PAN, Q., LIN, L., SZULWACH, K. E., SONG, C. X., HE, C., WU, H., WARREN, S. T., JIN, P., DUAN, R. & LI, X. 2012. Genome-wide DNA hydroxymethylation changes are associated with neurodevelopmental genes in the developing human cerebellum. *Hum Mol Genet,* 21**,** 5500-10.

WILLIAMS, E. C., ZHONG, X., MOHAMED, A., LI, R., LIU, Y., DONG, Q., ANANIEV, G. E., MOK, J. C., LIN, B. R., LU, J., CHIAO, C., CHERNEY, R., LI, H., ZHANG, S. C. & CHANG, Q. 2014. Mutant astrocytes differentiated from Rett syndrome patients-specific iPSCs have adverse effects on wild-type neurons. *Hum Mol Genet*.

YAMANAKA, S. 2007. Strategies and new developments in the generation of patient-specific pluripotent stem cells. *Cell Stem Cell,* 1**,** 39-49.

YU, J., VODYANIK, M. A., SMUGA-OTTO, K., ANTOSIEWICZ-BOURGET, J., FRANE, J. L., TIAN, S., NIE, J., JONSDOTTIR, G. A., RUOTTI, V., STEWART, R., SLUKVIN, II & THOMSON, J. A. 2007. Induced pluripotent stem cell lines derived from human somatic cells. *Science,* 318**,** 1917-20.

YU, N. K., BAEK, S. H. & KAANG, B. K. 2011. DNA methylation-mediated control of learning and memory. *Mol Brain,* 4**,** 5.

ZIGMAN, W. B. 2013. Atypical aging in down syndrome. *Dev Disabil Res Rev,* 18**,** 51-67.

ZIGMAN, W. B., SCHUPF, N., SERSEN, E. & SILVERMAN, W. 1996. Prevalence of dementia in adults with and without Down syndrome. *Am J Ment Retard,* 100**,** 403-12.

Appendices

Figure A1 | Controls for ICC staining.

Note: Positive control tissues was not available for the large array of antibodies used for this project, either because of inaccessibility of highly specific positive control tissue or limited funds for purchase of these expensive tissue samples. Secondary only stains were used as negative controls as shown below.

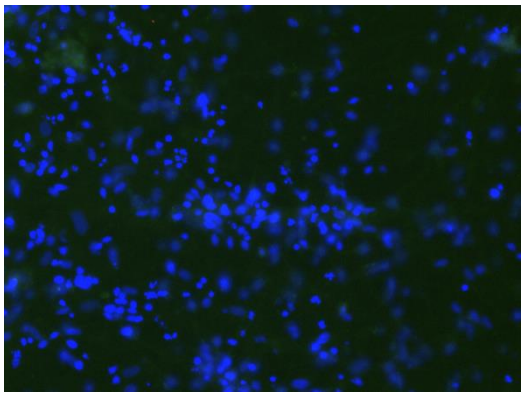

A shows secondary only staining with Ms IgG 488nm and Rb IgG 568nm, mounted with ProLong Gold Antifade Reagent with DAPI (Life Technologies).

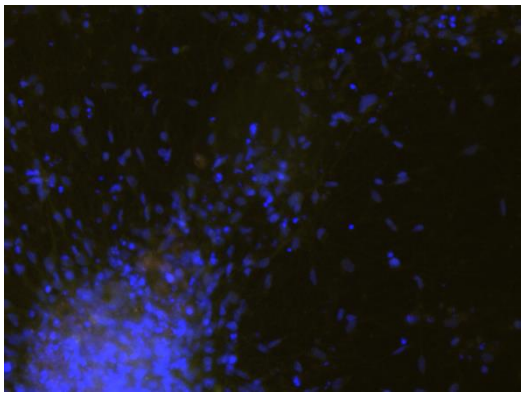

B shows secondary only staining with Ms IgM 488nm and Rb IgG 568nm, mounted with ProLong Gold Antifade Reagent with DAPI (Life Technologies).